Masteroppgave

NTNU
Norges teknisk-naturvitenskapelige universitet
Fakultet for ingeniørvitenskap
Institutt for marin teknikk

Thomas Hannasvik

Experimental Investigation of Beach Efficiency for Regular Waves

Masteroppgave i Marine Hydrodynamics
Veileder: Trygve Kristiansen
Juli 2019

NTNU
Kunnskap for en bedre verden

NTNU – Trondheim
Norwegian University of
Science and Technology

Experimental Investigation of Beach Efficiency for Regular Waves

Master Thesis, Marine Hydrodynamics

Norwegian University of Science and Technology

Author:

Thomas Hannasvik

Supervisor:

Professor

Trygve Kristiansen

July 11, 2019

Preface

This thesis is the concluding work of my Master of Science degree at the Department of Marine Technology at NTNU Trondheim.

First I would like to thank my supervisor Trygve Kristiansen for good academic advice and also for keeping me motivated and positive during challenging periods.

I would also like to thank the lab technicians at NTNU for constructing a perforated beach for me and helping me with my experiments. Bernard Molin also deserves a great thanks for academic input during my work.

Finally, I would sincerely like to thank all of my class mates at Marine Technology for all the fun we have had during these years, and give a special thank you to my good friends in office A2.015 (a.k.a President Office) for keeping my spirit up and for all the great laughs!

Abstract

A controlled and well-defined environment is important for reliable results in model testing. Wave absorption is, therefore, an important but often forgotten part of experiments. The aim of this study is to increase the understanding of wave reflection from beaches in wave tanks and collect data for optimization of wave absorption beaches.

Three experiments were conducted in this study: a comparison experiment of a non-perforated parabolic beach and a similar beach with 7.07 % perforation; a more comprehensive experiment of the perforated beach and an experiment in finite water conditions. Experiments one and two were done in the Lader Wave Laboratory and the third was done in the small towing tank, both at IMT, Tyholt.

In the first experiment three beach heights were tested for both beaches; surface piercing beach, beach tangential to waterline and submerged beach. Wave periods varied between 0.85 s and 1.71 s for three different steepnesses. Results showed that the perforated beach was more efficient than the non-perforated beach for all beach heights with a 52.4 % lower mean reflection coefficient. The difference was larger for the highest beach position (109 %) and smaller for the lower beach position (1.7 %).

In the first experiment, three beach heights were tested for both beaches: a surface piercing beach; a beach tangential to the waterline and a submerged beach. Wave periods varied between 0.85 s and 1.71 s for three different steepnesses. Results showed that the perforated beach was more efficient than the non-perforated beach

for all beach heights with a 52.4 % lower mean reflection coefficient. The difference was larger for the highest beach position (109 %) and smaller for the lower beach position (1.7 %).

In experiment number three, wave periods ranged from 0.57 s to 2.14 s and the water depth was close to halved relative to that of experiments one and two. The results in experiment three cannot be quantitatively compared directly to experiment two, but similar results for finite water conditions were observed. Observations show that the reflection coefficient is increasing with increased wavelength, and the beach is most efficient for the steepest waves, especially for the longer waves. However, the reflection coefficients deviated more compared to deep water conditions, and a repeated pattern was observed, which might be caused by parasitic waves.

Sammendrag

Et kontrollert og veldefinert miljø er viktig for å få pålitelige resultater i modellforsøk. Bølgeabsorbering er derfor en viktig, men også ofte glemt del av eksperimenter. Hensikten med denne studien er å øke forståelsen av bølgerefleksjon for strender i bølgetanker og samle data for optimering av bølgeabsorbsjonsstrender.

Tre eksperimenter ble gjennomført under denne studien: et sammenligningseksperiment av en ikke-perforert strand og en strand med 7.07 % perforering; et mer omfattende eksperiment for den perforerte stranden og et eksperiment med endelig vanndyp. Eksperiment én og to ble utført i Ladertanken og det tredje i den lille slepetanken, begge på IMT, Tyholt.

I det første eksperimentet ble tre forskjellige strandhøyder testet for begge strendene. Bølgeperiodene varierte fra 0.85 s til 1.71 s for tre forskjellige steilheter. Resultatene viste at den perforerte stranden var mer effektiv enn den ikke-perforerte stranden for alle strandhøydene, med gjennomsnittlig 52.4 % lavere refleksjonskoeffisient. Forskjellen var større for den høyeste strandposisjonen (109 %) og mindre for den lave strandposisjonen (1.7 %)

Under eksperiment nummer to ble den perforerte stranden testet i fem strandhøyder med bølgeperioder fra 0.57 s til 1.71 s. Refleksjonskoeffisientene ble utregnet ved hjelp av to forskjellige metoder. Metodene korrelerte godt for bølgelengdene som ble vektlagt, altså for bølger lengre enn stranden på 1.8 m ($T > 1.07$ s). Effekten av stranden minket for økende bølgelengder over 1.8 m for alle strandhøydene. For disse bølgene var effektiviteten til stranden strengt økende for lavere strandhøyder og steilere bølger. Den gjennomsnittlige refleksjonskoeffisienten ble redusert 46

% ved å senke stranden 50 mm og refleksjonskoeffisienten var i alt 25 % lavere for de steileste bølgene sammenlignet med de minst steile bølgene.

I eksperiment tre ble bølgeperioder fra 0.57 s til 2.14 s brukt og vanndypet omtrent halvparten av det i eksperiment én og to. De kvantitative resultatene i dette eksperimentet kan ikke sammenlignes direkte med eksperiment to, men lignende resultater ble funnet for forhold med endelig vanndyp. Observasjoner viser at refleksjonskoeffisienten øker med økende bølgelengde og at stranden er mer effektiv for bølgene med høyest steilhet, spesielt for de lengre bølgene. Likevel varierer refleksjonskoeffisienten mer under disse forholdene sammenlignet med resultatene i dypt vann, og repeterende mønstre er observert, noe som muligens skyldes parasittbølger.

Table of Contents

CHAPTER 1

Introduction

Despite increasingly advanced numerical methods, model testing still has a very important place in the development of marine technology. Model testing mainly have three different aims; to achieve design data to verify performance of different structures, to verify and calibrate theoretical methods and numerical codes, and to obtain better understanding of physical problems. These aims require a controlled and well-defined environment for reliable results, which is easier to acquire without waves reflecting from the tank walls. Some type of wave absorption device is therefore often installed in wave tanks to minimize wave reflection, where beaches are most common. However, the effectiveness of a beach depends on a number of parameters, such as wave period, wave height and beach geometry.

The objective of this thesis it to investigate how the beach efficiency is affected by changing of said parameters. The investigation will be done experimentally with three separate experiments. Experiment number one will be a comparison experiment of the non-perforated beach in the Lader Wave Laboratory and a newly constructed perforated beach with the same geometry. The second experiment is a broader study of the perforated beach in the Lader Wave Laboratory. The final experiment will be a finite water experiment done in the small towing tank.

Reflection coefficients from the measurement series will be calculated using two methods; a least squares method developed by Mansard and Funke, and a method

first described by Goda and Suzuki. The reflection coefficients should be compared for a number of wave periods, wave steepnesses and beach heights for both a non-perforated and a perforated beach. A visual study should also be done.

The second chapter in this thesis is some basic wave theory needed for further calculations and description of the two methods used. Chapter three is a short overview of how the analysis procedure was done in MATLAB. The experiment set up is described in chapter four together with conducting of the experiments. The results are presented in chapter five, before being discussed in chapter six and concluded in chapter seven.

The waves in this thesis were first defined as full scale waves and later scaled down to 1:49 in model scale. The full scale wave periods and model scale wave periods are therefore both used throughout this thesis. The calculated reflection coefficients are however non-dimensional which makes the scale unimportant as long as the waves are scaled correctly.

CHAPTER 2

Theory

Some of the following theory is well known and can be found in many textbooks but a short repetition is needed to explain the methods implemented later in this thesis.

2.1 Regular Wave Theory

Starting with basic wave theory, the surface elevation for regular/linear wave propagating in the positive x-direction is given by [1]

$$\zeta(x,t) = \zeta_A \cos(kx - \omega t) \tag{2.1}$$

where ζ_A is the wave amplitude, k is the wave number and ω is the wave frequency.

The wave frequency is then given by

$$\omega = \frac{2\pi}{T} \tag{2.2}$$

The wave number, k can be found by the dispersion relation which is given by

$$\omega^2 = kg \tanh kh \tag{2.3}$$

Deep water is assumed when the water depth, h is larger than half of the wave length, λ.

The wave length is related to the wave number by $k = \frac{2\pi}{\lambda}$.

The wave (phase) velocity is given as

$$c_W^2 = \frac{g\lambda}{2\pi} \tanh kh \tag{2.4}$$

The group velocity is then expressed as

$$c_G = \frac{c_W}{2}(1 + \frac{2k}{\sinh 2kh}) \tag{2.5}$$

Steepness of waves can be calculated by

$$\frac{H}{\lambda} = s \tag{2.6}$$

where H is the wave height, also known as $2\zeta_A$

When scaling waves from full scale to an experiment with a scale of 1:x, the wave period can be calculated as

$$T = \frac{T_{FS}}{\sqrt{x}} \tag{2.7}$$

where T_{FS} is the full scale wave period.

2.2 Wavemaker Theory

For wavemakers, the ratio between stroke amplitude and wave height is a function of wave period, water depth and wakemaker type [2].

The stroke to wave height ratio for a piston wavemaker is given by

$$\frac{H}{S} = \frac{2(\cosh\ 2k_p h - 1)}{\sinh\ 2k_p h + 2k_p h} \tag{2.8}$$

The stroke to wave height ratio for a wavemaker with a hinged flap is given by

$$\frac{H}{S} = 4\,\frac{\sinh(kh)}{kh_{wm}}\,\frac{kh_{wm}\,\sinh(kh) + \cosh(kh - kh_{wm}) - \cosh(kh)}{\sinh(2kh) + 2kh} \tag{2.9}$$

where h_{wm} is the height from the wavemaker hinge to the free surface.

2.3 Measurement of Wave Reflection

The most common way to quantify wave reflection is the reflection coefficient. It is the ratio of the amplitude of the reflected wave and the incident wave. To separate the amplitudes of the incident and reflected wave from the measurement series different methods have been developed. In this thesis two methods will be applied to calculate the wave reflection from a beach. The first method which is the main method used in the experiments is a least squares method which minimizes the error function, first described by Mansard and Funke (1980) [3]. Method number two was first described by Goda and Suzuki (1976) [4]. Both methods are also described in detail by Isaachson (1991) [5].

Least Squares Method

By applying the least squares method three wave probes are used in the experiments. Five quantities were measured; the wave amplitude at the three wave probes, A_1, A_2 and A_3, and the phase difference between probe 1 and 2, δ_2, and 1 and 3, δ_3. The distance between the probes is known and can be written in dimensionless form as $\Delta_n = k\lambda_n$, where k is the wave number and λ is the distance from the first probe to probe n. The amplitude of the incident and reflected wave may now be expressed as:

$$a_i = |X_i| \qquad a_r = |X_r| \tag{2.10}$$

where

$$\begin{aligned} X_i =& \frac{s_2 s_3 - 3 s_4}{s_5} \\ X_r =& \frac{s_1 s_4 - 3 s_3}{s_5} \end{aligned} \tag{2.11}$$

and

$$\begin{aligned} s_1 =& \sum_{n=1}^{3} \exp(i 2 \Delta_n) \\ s_2 =& \sum_{n=1}^{3} \exp(-i 2 \Delta_n) \\ s_3 =& \sum_{n=1}^{3} A_n \exp[i(\delta_n + \Delta_n)] \\ s_4 =& \sum_{n=1}^{3} A_n \exp[i(\delta_n - \Delta_n)] \\ s_5 =& s_1 s_2 - 9 \end{aligned} \tag{2.12}$$

The reflection coefficient is given as

$$K = \frac{a_r}{a_i} \tag{2.13}$$

Goda's Method

In Goda's method only two wave probes are needed and three quantities are measured; the wave amplitude at the two probes wave probes, A_1 and A_2, and the phase difference between probe 1 and 2, δ_2.

The amplitude of the incident and reflected waves can now be calculated as

$$a_i = \frac{1}{2|\sin k\Delta l|}\sqrt{A_1^2 + A_2^2 - 2A_1A_2\cos(\Delta + \delta)} \tag{2.14}$$

$$a_r = \frac{1}{2|\sin k\Delta l|}\sqrt{A_1^2 + A_2^2 - 2A_1A_2\cos(\Delta - \delta)} \tag{2.15}$$

$$\tag{2.16}$$

where $\Delta = \Delta_2$ and $\delta = \delta_2$

The reflection coefficient is given as

$$K = \frac{a_r}{a_i} \tag{2.17}$$

CHAPTER 3

Analysis

3.1 Analysis in MATLAB

For each experiments a MATLAB code was used to generate an input file for the wavemaker with desired wave periods and steepnesses. The measurements were made using catmanAP V5.1.1 software with a sampling frequency of 200 Hz and a butterworth filter with 10 % of the sampling frequency, 20 Hz. The bin-files containing data from the measurement series were processed in MATLAB.

Measurement series

For all three experiments a measurement series of the wave elevation was made for every beach position. Figure 3.1 shows an example of such a series measured by one of the wave probes. This series consists of eight wave periods with three different wave steepnesses, making a total of 24 different wave conditions. It is clear that the wave amplitude increases gradually for eight wave conditions and then decreases before gradually increasing again. Here the first eight wave conditions are all the wave periods for the least steepest waves. The next eight wave conditions are the same wave periods but with increased steepness. The eight remaining wave

conditions are the steepest waves. The period between each wave condition was set to 180 seconds.

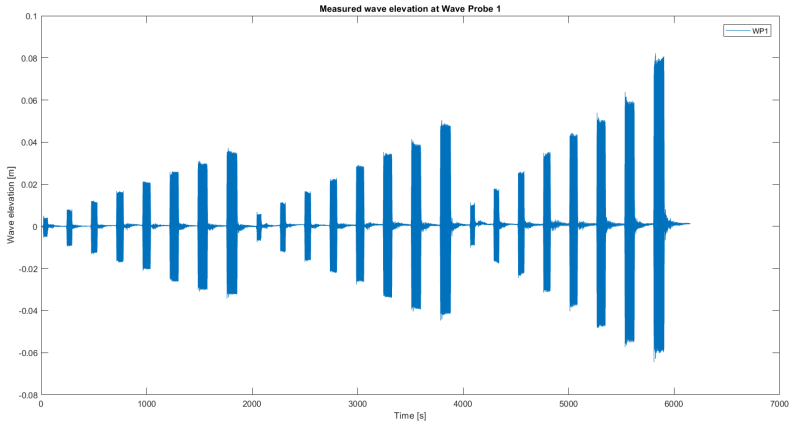

Figure 3.1: Example of a measurement series of wave elevation for waves with eight different wave periods and three different steepnesses.

By enlarging one of the wave conditions displayed in Figure 3.1 the individual waves can be seen. Figure 3.2 shows the wave height of the individual waves for each of the total 60 waves. One can also clearly see the effect of the ramp-up function of the wavemaker.

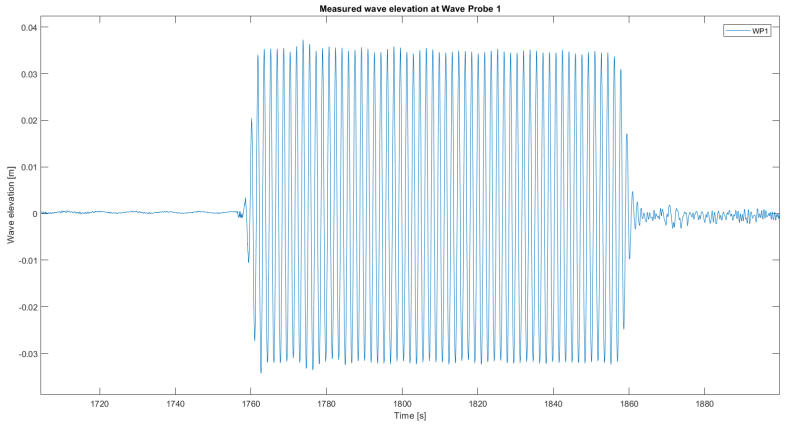

Figure 3.2: Enlarged part of the measurement series showing all individual waves for a wave condition, here with a wave period of $\frac{12}{7}$ s and with steepness $\frac{1}{60}$.

Dividing the measurement series in intervals

To enable an analysis of each individual wave condition the measurement series must be divided into intervals consisting of the measured wave elevation for one condition. The interval windows were found automatically. By detecting the local maximums and local minimums (the wave crests and wave troughs) the beginning of each interval could be defined as 2000 samples earlier than the first local maximum after a period of 10 000 samples without a local maximum. The end of each interval was defined in a similar way as 5000 samples after the previous local maximum after a period of 10 000 sample without a local maximum.

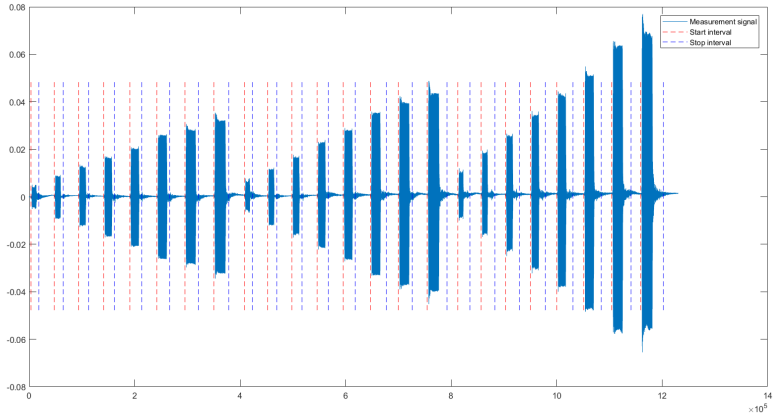

Figure 3.3: The measurement series is divided into intervals where each interval contains one wave condition.

For each interval, the wave period is found by determining the mean number of sample points between each local maximum multiplied with the sampling frequency. This is done for all three wave probes and a mean wave period is calculated. The waves created during the ramp-up of the wavemaker were excluded.

Filtering

The measurement series is filtered with a bandpass filter around the first order harmonic. The lower cut-off frequency is set to 0.9 times the wave frequency [Hz] found from the mean wave period, while the upper cut-off frequency is set to 1.1 times the wave frequency. In Figure 3.4 the filtering is illustrated for the largest waves where the second and third order harmonic is most present. Note

that the amplitude of the bandpass filter is 1 although illustrated otherwise in the figure.

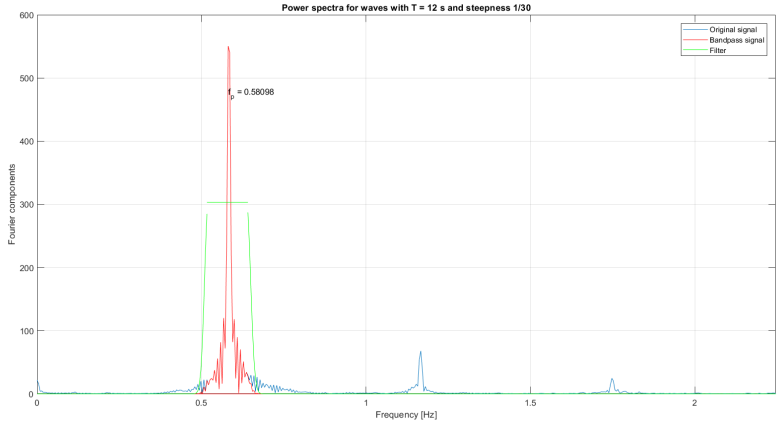

Figure 3.4: Illustration of a bandpass filter around the first order harmonic with cut-off frequencies of 0.9 and 1.1 times f_p

Figure 3.5 shows a comparison of the unfiltered and filtered measurement series. Notice that the wave crest is smaller and the wave trough deeper for the filtered series.

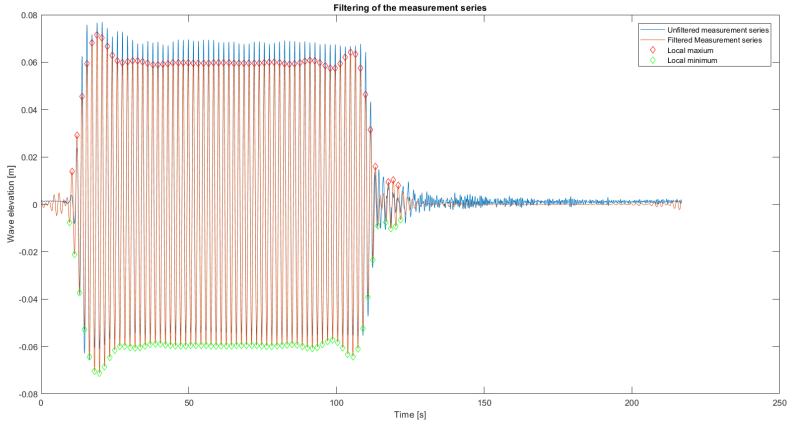

Figure 3.5: The filtered time series compared to the measured time series pre-filtering.

Finding the time window for analysis

For calculating the amplitude of the incident and reflected wave, the time window for measurement is important. The time window of interest in the measurement series is when only these two waves are present. The beginning of this time window should be when the first wave after the ramp-up waves reaches the wave probe nearest the wavemaker after being reflected from the beach. The end on the time window should be when this reflected wave again reaches the same wave probe after being re-reflected from the wavemaker. For the smaller waves, the waves will not be re-reflected until after the end of the incident wavetrain has reached the wave probe. In that case the end of the time window is set to 10 wave periods earlier than the last registered wave. The red and blue lines in Figure 3.6 represents the beginning and end of this time window for the largest waves.

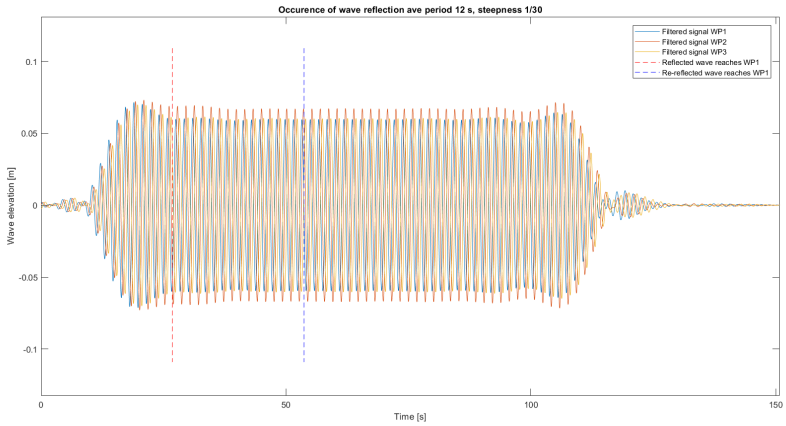

Figure 3.6: Calculations of reflection should only be done while the incident and reflected wave is present and before re-reflection occurs. The time window of interest is illustrated between the dashed red line and the dashed blue line.

Calculating the reflection coefficient

Now that the measurement series is filtered and the correct time window is found, the wave amplitudes measured at all three wave probes are easily found within this window by locating the local maximums. The phase difference is found as described in the theory. The probe distances are known from the experimental set-up and is made non-dimensional by multiplying the probe distance with the wave number, k. The amplitudes of the incident and reflected waves can from these

parameters be found as described in Section 2.3. The ratio between them is the reflection coefficient.

CHAPTER 4

Experiments and Observations

Three experiments were done during this study. Two of them were done in the Lader Wave Laboratory. The first experiment was a comparison study between a perforated beach and a non-perforated beach while the second experiment was a more in-depth study of the perforated beach. These were mainly deep water tests. The third and last experiment was done in the Small Towing Tank to check if the results found in the deep water conditions should be representative for finite water conditions in terms of trends. The results could not be directly compared in terms of magnitude. Both the Lader Wave Laboratory and the Small Towing Tank is located at NTNU, Department of Marine Technology at Tyholt.

4.1 Equipment and Set Up

Lader Wave Laboratory

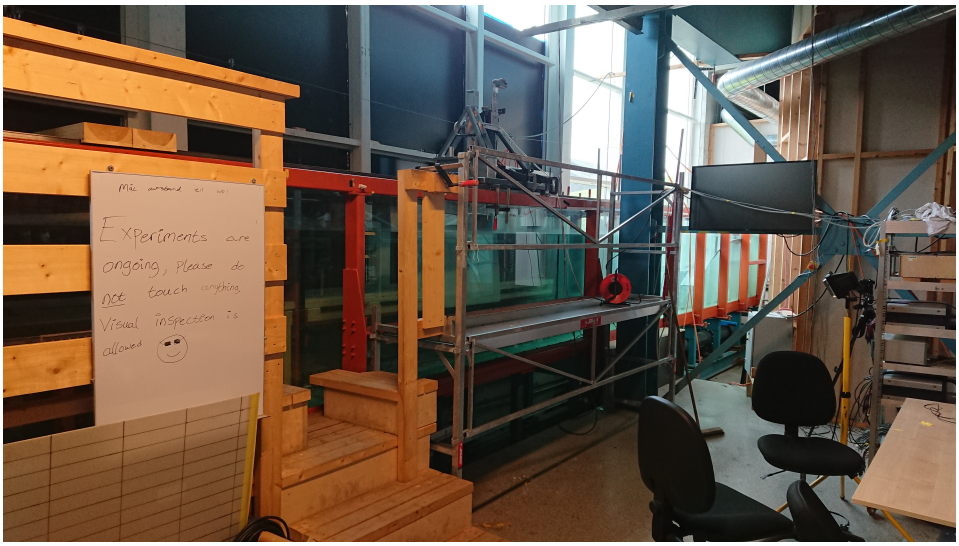

Figure 4.1: A picture of the Lader Wave Laboratory.

As seen in Figure 4.2, the Wave Lab is 13.60 meters long and 0.60 meters wide with a draught of 1.00 meter. In one end there is a flap wavemaker which is hinged 0.11 meters above the bottom of the tank. The wavemaker motion is measured with a sensor placed 0.3 meters from the wavemaker. In the other end of the tank, we find a parabolic beach. The approximated geometry of the beach is shown in Figure 4.3. Behind the beach, a perforated surface-piercing cylinder is placed with a diameter of 220 mm. This is the inlet for a pump which can transport water from the beach end to the wavemaker end to create a current in the tank. This pump was not used in this experiment, although the cylinder might affect the results. This will, however, be discussed later. Between the wavemaker and the beach, three calibrated wave probes were placed at 7.96 meters, 8.45 meters, 9.36 meters from the wavemaker's mean (zero) position. The probes are located in the middle of the tank, at y = 0.30 meters.

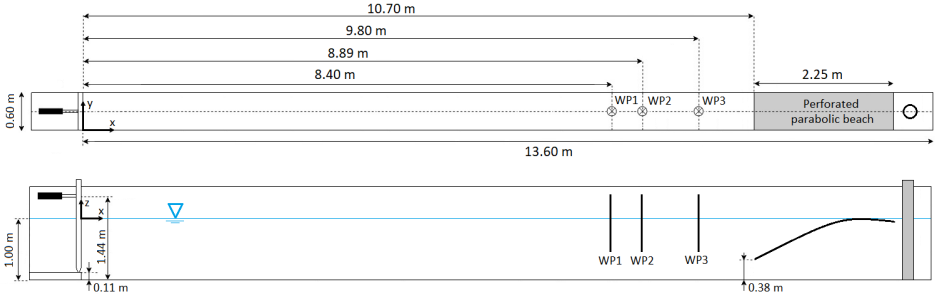

Figure 4.2: Test set up for experiment in the Lader Wave Laboratory with a hinged flap wavemaker, three wave probes and a perforated parabolic beach. A non-perforated beach was also used in one experiment.

A coordinate system was established with its centre at the wavemaker's mean (zero) position, at the free surface and at the right-hand side of the tank when looking from the wavemaker in the incident wave propagation direction. The positive x-direction is defined in the direction of wave propagation, the positive y-direction is defined towards the left-hand side wall and the positive z-position is defined upwards, opposite of the gravitational acceleration.

Both the non-perforated beach and the perforated beach in the Lader Wave Laboratory had the same geometry. The porosity of the perforated beach is 7.07 %. The highest point of the beach is located at 1.80 meters from the start of the beach. Notice that this is the defined beach length in the calculations. The total length of the beach is approximately 2.25 meters, and it is located 0.38 meters above the tank bottom when the top of the beach is in the mean water line (at z = 0). The z-position of the beach was measured for every 10 cm in the x-direction in an attempt to find the beach geometry. The result is shown in Figure 4.3, where the origin is located at the beach end closest to the wavemaker.

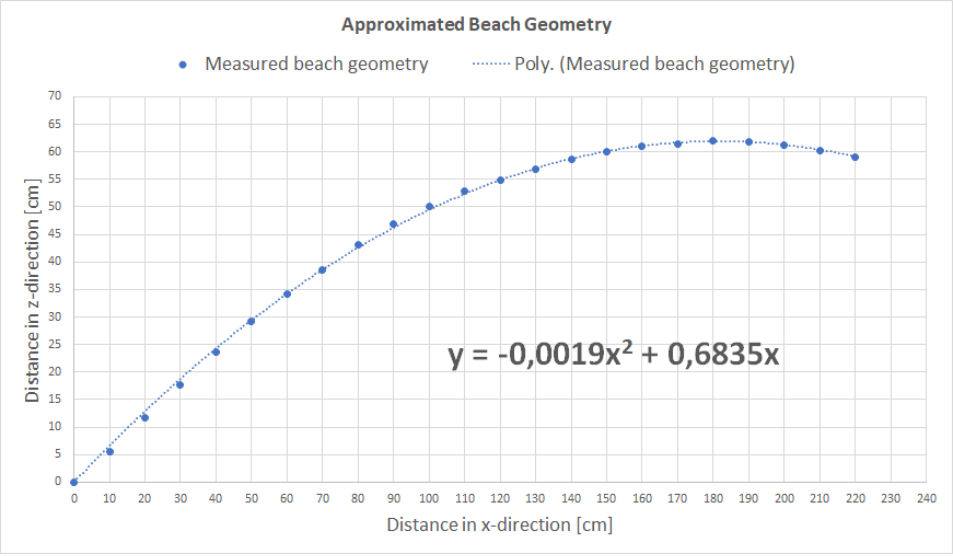

Figure 4.3: A second degree polynomial curve fit was used to approximate the beach geometry of perforated beach in the Lader Wave Laboratory from the measured coordinates.

By differentiation of the curve fit formula, the beach slope in the mean waterline could be calculated for the beach heights used in the experiments and are shown in Table 4.1.

z-position of top of beach	0.025	0.010	0.000	-0.010	-0.025
Beach slope at mean water line	7.55°	4.32°	0°	N/A	N/A

Table 4.1: The calculated beach slope in the mean waterline for the approximated beach geometry.

Small Towing Tank

As seen in Figure 4.4, the Small Towing Tank is approximately 25 meters long and 2.5 meters. For this experiment, the deepness was set to 0.55 meters. In one end there is a piston wavemaker and in the other end a perforated parabolic beach. The beach had a varying degree of perforation with 12 % perforation on the first half, going all the way from the tank bottom up to about 0.3 meters. It had a perforation of 8 % in the top half. The top of the beach was located 0.01 meters below the mean free surface during these experiments. Between the wavemaker and the beach, eight calibrated wave probes were placed in pairs at 15.26 meters, 15.69 meters, 15.97 meters and 16.49 meters from the wavemaker's mean (zero)

position. The probes are located in the 0.25 meters from the centre line of the tank in the wave propagation direction. A coordinate system was established in the same way as the experiments in the Lader Wave Laboratory.

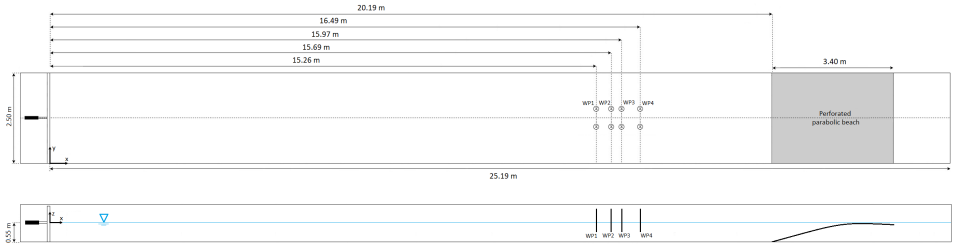

Figure 4.4: Test set up for experiment in the Small Towing Tank.

The beach geometry was approximated in the same way as the beach in the Lader Wave Laboratory, but with fewer measurement points, making the approximated geometry more uncertain. The approximation is shown in Figure 4.5, and by using the curve fit formula, the beach slope in the mean waterline in this experiment was found to be 1.53°.

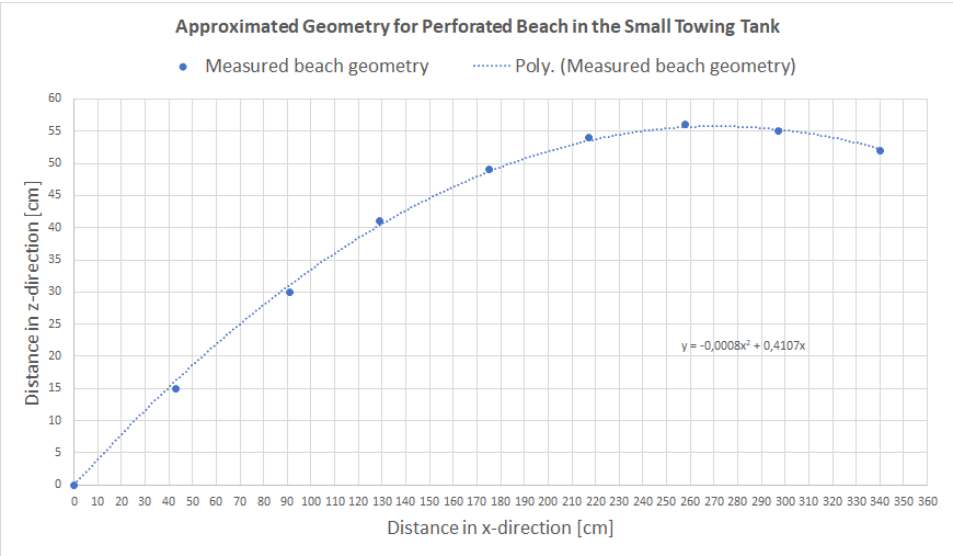

Figure 4.5: Approximated beach geometry of perforated beach in the Small Towing Tank.

Wave Probes and Positioning of Wave Probes

The sensors (wave probes) measuring the wave elevation consisted of two rods about 20 mm apart, each electrically conductive. When these rods enter the water, the current is short-circuited and one can measure the voltage in the circuit. A deeper draught of the sensor leads to less resistance and therefore a higher voltage. Two different types of wave probes were used, one type for the experiments in the Lader Wave Laboratory and another for the experiment in the Small Towing Tank, see Figure 4.6.

Figure 4.6: The two types of wave probes used. The upper wave probe type was used for the experiment in the Small Towing Tank and the lower wave probe type was used for the experiments in the Lader Wave Laboratory. The lower one was found to be the most accurate.

For wave probe positioning, some considerations had to be made. For the least squares method, the distance between the wave probes should be such that a parameter defined as $\mu = \frac{\Delta_3}{\Delta_2}$ and values of $\mu \approx 0.45$ or $\mu \approx 0.65$ should be most suitable for wavelengths no shorter than one-third of the total probe distance [5]. The probe distances were then found by choosing a total probe distance of less than three times the wavelength of the shortest waves and then calculating Δ_3 and finding Δ_2 leading to a ratio of $\mu = 0.65$. For Goda's method, calculations fail when the probe distance is equal to an integer number of half wavelengths. It is recommended that tests shouldn't be carried out for $0.4L < \lambda_2 < 0.6L$, where λ_2 is the distance between probe 1 and probe 2.

Another thing taken into consideration is the distance from the wave probes to the beach. The wave probes should be located far enough from the beach to minimize nonlinear effects from the breaking of the waves. Goda and Suzuki suggest that

the last wave probe could be set as near as $0.2L$ from the reflective face for regular waves [4]. The first wave probe should be placed close enough to the beach so that the interaction of reflected and incident waves can be measured by the probes. This is mainly an issue for the shortest waves which propagate the slowest. The coordinates of all the wave probes from the experiments are given in Table 4.2, 4.3 and 4.4.

Wave Probe #	WP 1	WP 2	WP 3
x-position [m]	6.00	6.79	7.86

Table 4.2: The x-position of the wave probes for experiment one in the Lader Wave Laboratory. Note that $\mu = 0.42$ for this experiment and not 0.65 which is used in experiment two and three.

Wave Probe #	WP 1	WP 2	WP 3
x-position [m]	8.40	8.89	9.80

Table 4.3: The x-position of the wave probes for experiment two in the Lader Wave Laboratory.

Wave Probe #	WP 1A	WP 1B	WP 2A	WP 2B
(x,y)-position [m]	(15.26, 1.00)	(15.26, 1.50)	(15.69, 1.00)	(15.69, 1.50)
Wave Probe #	WP 3A	WP 3B	WP 4A	WP 4B
(x,y)-position [m]	(15.97, 1.00)	(15.97, 1.50)	(16-49, 1.00)	(16.49, 1.50)

Table 4.4: The (x,y)-position of the wave probes for experiment three in the Small Towing Tank.

4.2 Calibration

Calibration of Wavemakers

The wavemakers, both the hinged wavemaker in the Lader Wave Laboratory and the piston wavemaker in the Small Towing tank, were found to have differences in the input signal and the output signal in terms of amplitude. Both wavemakers had the largest difference between input and output for the smallest amplitudes. To account for this, mechanical transfer functions had to be established. In Figure 4.7 the mechanical transfer function for the flap wavemaker is shown. It can be seen that the transfer function gradually decreases before stabilizing around 1.93 for

wave periods higher than 1 second (7 seconds in full scale). The transfer function was almost similar for the three steepnesses.

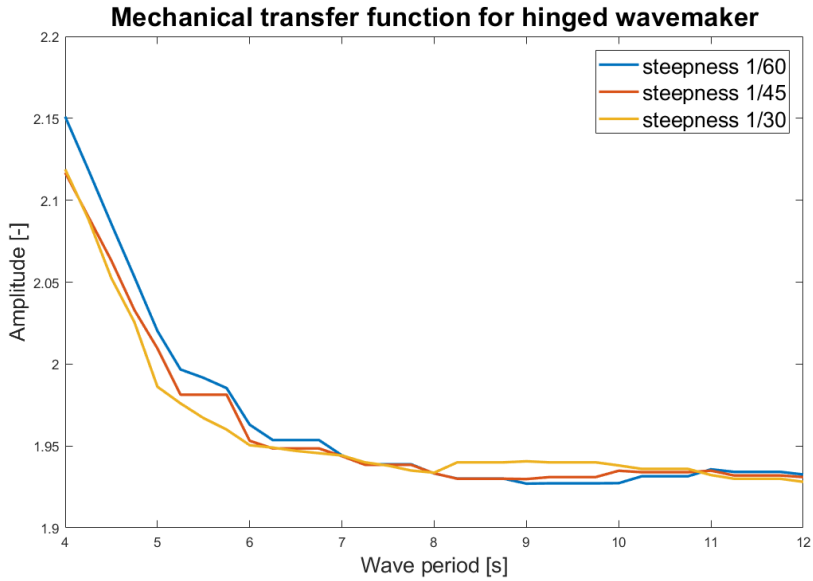

Figure 4.7: The mechanical transfer function for the wavemaker in the Lader Wave Laboratory. Note that the wave periods in this figure is corresponding to full scale wave periods.

After multiplying the input wave amplitude with the transfer function, it was found that the input and output signals were close to identical. The output signal was found to be 0.18 % higher than the input signal using a linear trendline which can be seen in Figure 4.8.

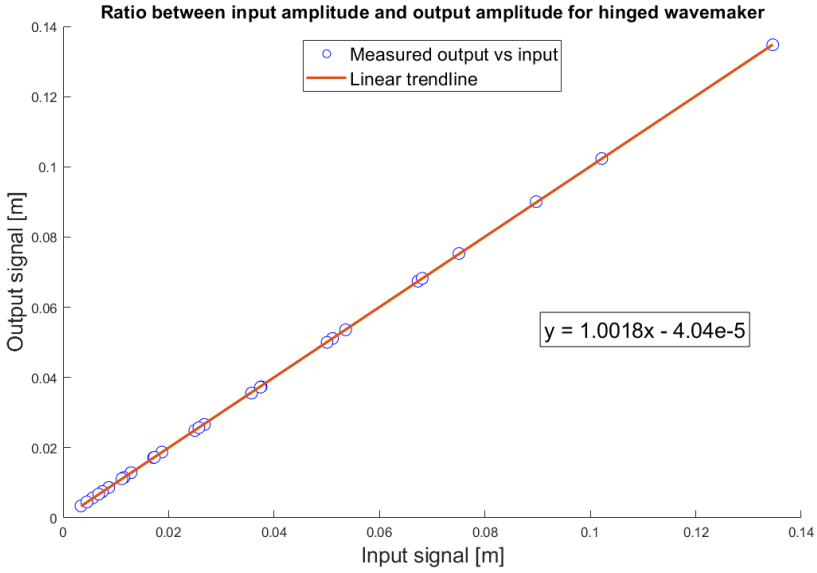

Figure 4.8: Comparison of the output signal and the input signal for the wavemaker in the Lader Wave Laboratory after taking correction with the mechanical transfer function.

A similar mechanical transfer function was established for the piston wavemaker and can be seen in Figure 4.9. Notice that the transfer function amplitude varies more with wave steepness compared to the hinged wavemaker. A larger transfer function for the lowest waves suggests that the wavemaker is more inaccurate for smaller amplitudes. Further, there is no difference in input and output for the larger waves.

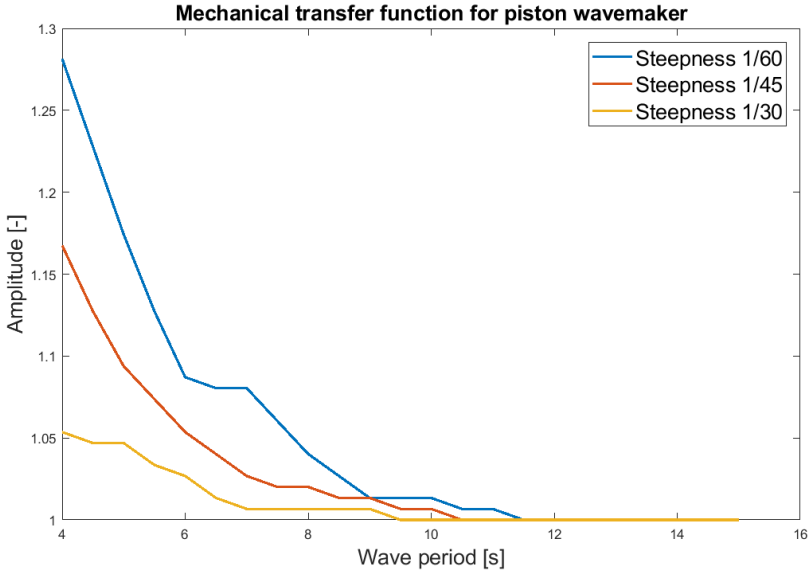

Figure 4.9: The mechanical transfer function for the wavemaker in the Small Towing Tank. Notice that the wave periods in this figure is corresponding to full scale wave periods.

Calibration of Wave Probes

Figure 4.10 shows the set up for a wave probe and how it was mounted in the Lader Wave Laboratory. The wave probes were calibrated by measuring the change in voltage for a known increase in the draught. The rod clamped to the transverse beam holding the wave probe had holes drilled every 20 mm, making the measuring of the draught easy. A total of eleven measurement points were made for each of the wave probes. The number of points used was due to the inaccuracy of the sensors, which is discussed further in Section 4.4. Most of the wave probes were precalibrated and only needed adjustments to the calibration factor. A calibration curve is shown in Figure 4.11. For this wave probe, the calibration factor had to be increased by 7.2 %. For troublesome wave probes, the measurements in the ± 100 mm range from the mean free surface were emphasized.

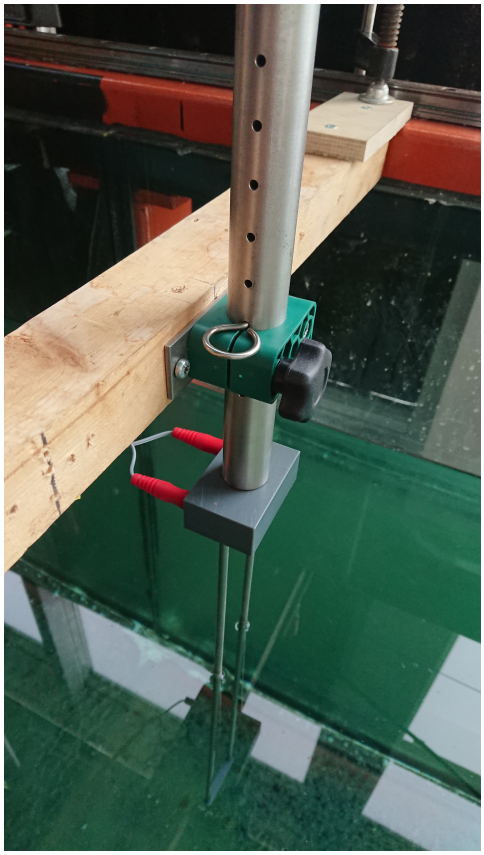

Figure 4.10: This set up for a wave probe shows the two partly submerged rods leading electricity, connection points for the data acquisition system and the rod for height adjustments clamped to the transverse beam supporting the wave probe.

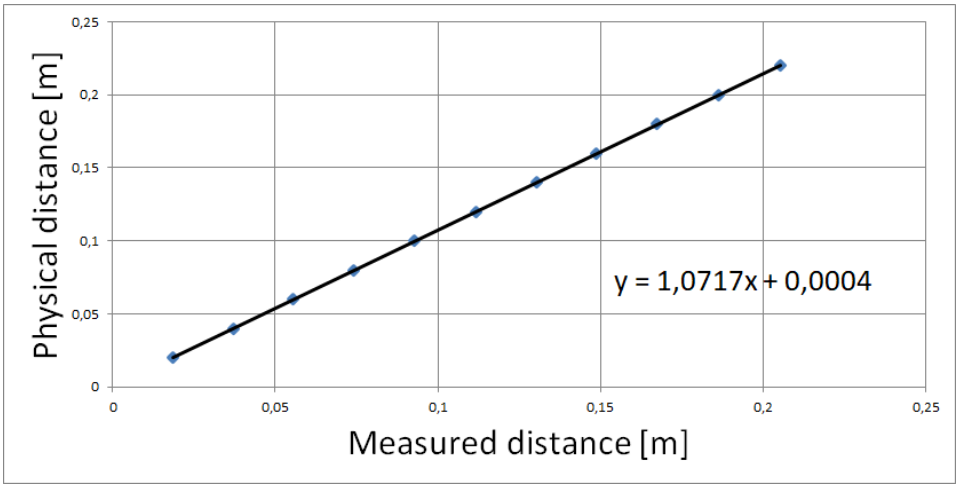

Figure 4.11: Calibration curve for a wave probe.

4.3 Experiments

All three experiments were done in 1:49 scale with wave periods ranging from 4 seconds to 15 seconds in full scale. The full-scale water depth for experiments done in the Lader Wave Laboratory is 49 meters and for the experiment in the Small Towing Tank 27 meters. Waves with periods greater than 12 seconds were only studied in the towing tank. This leads to wave periods and wavelengths in model scale according to Table 4.5. Not all wave periods are included in the table, only integer wave periods in full scale.

$T_{FS}[s]$	$T_{MS}[s]$	$\lambda_{FS}[m]$ (d.w.)	$\lambda_{MS}[m]$ (Lader)	$\lambda_{MS}[m]$ (Towing)
4	0.57	24.98	0.51	0.51
5	0.71	39.03	0.80	0.80
6	0.86	56.21	1.15	1.14
7	1.00	76.50	1.56	1.53
8	1.14	99.92	2.03	1.93
9	1.29	126.47	2.54	2.33
10	1.43	156.13	3.08	2.72
11	1.57	188.92	3.62	3.11
12	1.71	224.83	4.16	3.48
13	1.86	263.86	-	3.85
14	2.00	306.02	-	4.22
15	2.14	351.29	-	4.58

Table 4.5: Comparison of wave periods and wavelengths in full scale and model scale for an experiment with scale 1:49. Subtext FS means full scale and MS means model scale. The full scale wavelengths are calculated using deep water assumptions.

Experiment One - Comparison Between Perforated Beach and Non-perforated Beach

The first experiment was a comparison study between a perforated beach and a non-perforated beach. A perforated beach was made for this purpose with the same geometry and dimensions as the non-perforated beach. Wave periods from T = 6 seconds to T = 12 seconds in full scale with 1-second increments were used in this study, corresponding to model scale wave periods from 0.86 seconds to 1.71 seconds. Three different wave steepnesses were applied; s = 1/60, s = 1/45 and s = 1/30, making a total of 21 different wave conditions. The water depth was 1 meter, meaning deep water conditions for wave periods under 8 seconds and transitional water for T = 8 seconds and greater.

Three different beach draughts were tested; with the waterline making a tangent line on the highest point of the parabolic beach (with the top of the beach at z = 0), with the whole beach being submerged by 20 mm (top of beach at z = -0.02) and with the beach partially submerged with the top of the beach at z = 0.02. This resulted in a total of 63 different cases.

Experiment Two - More in-depth Study of Perforated Beach

In experiment number two, the perforated beach was used again as data from more wave periods and beach positions was of interest. The wave periods in this experiment ranged from T = 4 seconds to T = 12 seconds in full scale with 0.25 seconds increments leading to 33 different wave periods. By using the same steepnesses as in experiment one, the resulting number of wave conditions was 99. The water depth was again set to 1 meter.

The beach draughts used for this experiment was with the top of the beach at z = 0.025, z = 0.01, z = 0, z = -0.01 and z = -0.025. The total number of cases tested was therefore 495.

During experiment number two, pictures were taken and some recordings were done of the wave train hitting the beach. This was done to help observe and document different flow phenomena occurring. A Casio EX-F1 digital camera with a high-speed function of 300 frames per second was used to capture the flow. The wave periods filmed were corresponding to 4, 5, 6, 7, 8, 9, 10, 11 and 12 seconds in full scale. Runs for all the three different steepnesses were filmed. This was done for four of the beach positions; with the top of the beach at z= 0.01, z = 0.00, z = -0.01 and z = -0.025.

Experiment Three - Study in Finite Water Conditions

The third experiment was done in a larger tank but with a water depth of only 0.55 meters. This was to check if the same trends found in the results for experiment one and two applied also for shallower water. Full scale wave periods from 4 seconds to 15 seconds were used with increments of 0.5 seconds. The same steepnesses were also used for this experiment, making a total of 69 wave conditions. The beach height was kept constant with the top of the beach submerged with 10 mm (top of beach at z = -0.01)

4.4 Accuracy and Reliability

Precision Error

Repeated runs for calculation of precision limit were done for both the perforated beach and the non-perforated beach in the Lader Wave Laboratory. The top of the beach was located at z = 0.00 and the largest waves were chosen for this test. The

reason for this is that the longest and steepest waves should have a greater chance of causing non-linear effects making the measurements deviate the most for these waves. Later it was experienced that the largest waves had the most consistent results and the precision error should be calculated for smaller waves.

In Figure 4.6 and Figure 4.7 the measured reflection coefficients are shown for the perforated beach and non-perforated beach respectively. The reflection coefficients are very consistent and notice that the wave period is very close to the desired wave period of 1.714 seconds. The precision errors can be found in Tables 4.6 and 4.7.

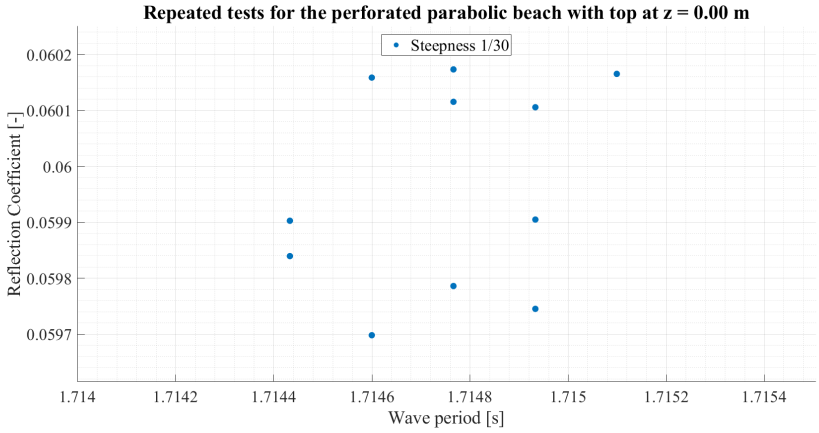

Figure 4.12: Reflection coefficients for 11 repeated tests for the perforated beach. Wave period was set to 12 seconds full scale (1.714 seconds in model scale) and the steepness 1/30.

	Value	Unit
Number of runs, N	11	-
Mean reflection coefficient, $\bar{X}$	0.05996	-
Precision limit, $P_{\bar{X}}$	0.000136	-
Uncertainty of reflection coefficient	0.22	%

Table 4.6: Precision limit of reflection coefficient for perforated beach.

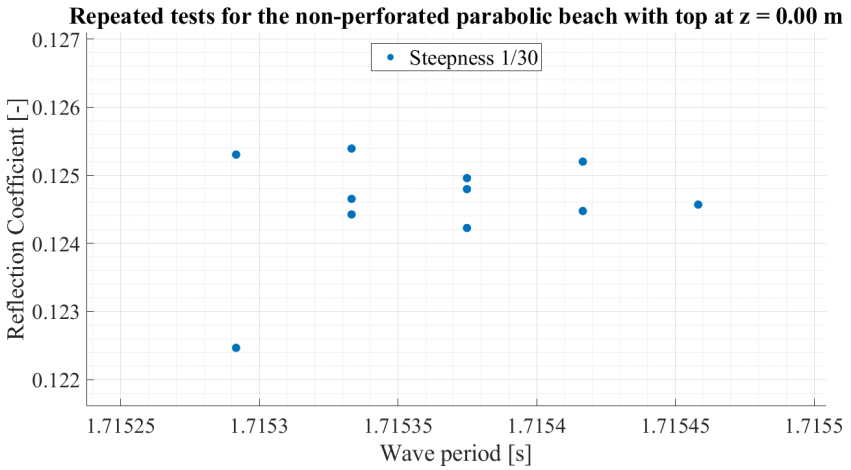

Figure 4.13: Reflection coefficients for 11 repeated tests for the non-perforated beach. Wave period was set to 12 seconds full scale (1.714 seconds in model scale) and the steepness 1/30.

	Value	Unit
Number of runs, N	11	-
Mean reflection coefficient, $\bar{X}$	0.1244	-
Precision limit, $P_{\bar{X}}$	0.000727	-
Uncertainty of reflection coefficient	0.58	%

Table 4.7: Precision limit of reflection coefficient for non-perforated beach.

Bias Error

The cylinder (pump inlet) behind the beach in the Lader Wave Laboratory will probably affect the results in experiment one and experiment two. This might be a larger source of error for the lower beach positions, as for the higher beach positions it can be assumed that more of the wave energy is absorbed from the beach. The cylinder will most likely lead to lower reflection coefficients compared to a similar wave tank with just a solid wall behind the beach. The reason is that the cylinder acts as a wave damper by contributing to vortex shedding and viscous dissipation. This effect is probably increased further because of its perforated walls. However, the effect of this remains unknown.

The wave probes used for measuring wave elevation in the Small Towing Tank seemed to have fluctuating measurements. There could be multiple reasons for

this, but they are hard to quantify. Some reasons could be water pollution, dust making a coating on the rods, electrical noise or temperature changes. The wave probes were said to have 2.5 % deviation for every 1 C° change of water temperature. This assumption is not documented but is consistent with my experiences. In addition, the water level was not totally steady, as there was some water drainage, especially in the small towing tank, zero-measurements were taken before each set of runs to minimize the effect. The wave probes used in the Lader Wave Laboratory were less troublesome and easier to calibrate.

Another error source is fouling in the tank, especially in the Lader Wave Laboratory. The tank hasn't been cleaned in a long time and fouling can be problematic, especially on a beach as this leads to a rougher surface and dissipation which can affect the results. This was probably affecting the run with the non-perforated beach the most, as the perforated beach was recently constructed and didn't have much fouling yet.

The beach position was a bit hard to get in the exact correct position. This beach height can be adjusted on both sides individually and a small difference in height on one of the sides will cause a canted beach which then can lead to the waves breaking on one side of the tank before the other. In addition the perforated beach was moving a little for the larger waves. Not the entire beach, but the perforated plate was rising approximately 2 mm between the welding points for every wave that passed.

Poor calibration can also be a source of error. The wave probes in the towing tank are fluctuating a bit and the calibration curves for some of the wave probes can be impossible to fit with a straight line. The wave probes were checked every morning to assure consistent measurement and deviations of more than 1.5 % was not experienced. The calibration of the wavemakers could also be done incorrectly, although this was double checked and less likely. The sensors measuring the amplitude of the wavemakers were precalibrated, probably a long time ago, and haven't been checked after the experiment.

4.5 Visual Observations

In this section some snapshots are shown from the recordings done during experiment number two. The purpose was to determine the time of occurrence for the breaking of a wave and how this was affected by change of beach height, wave period and wave steepness.

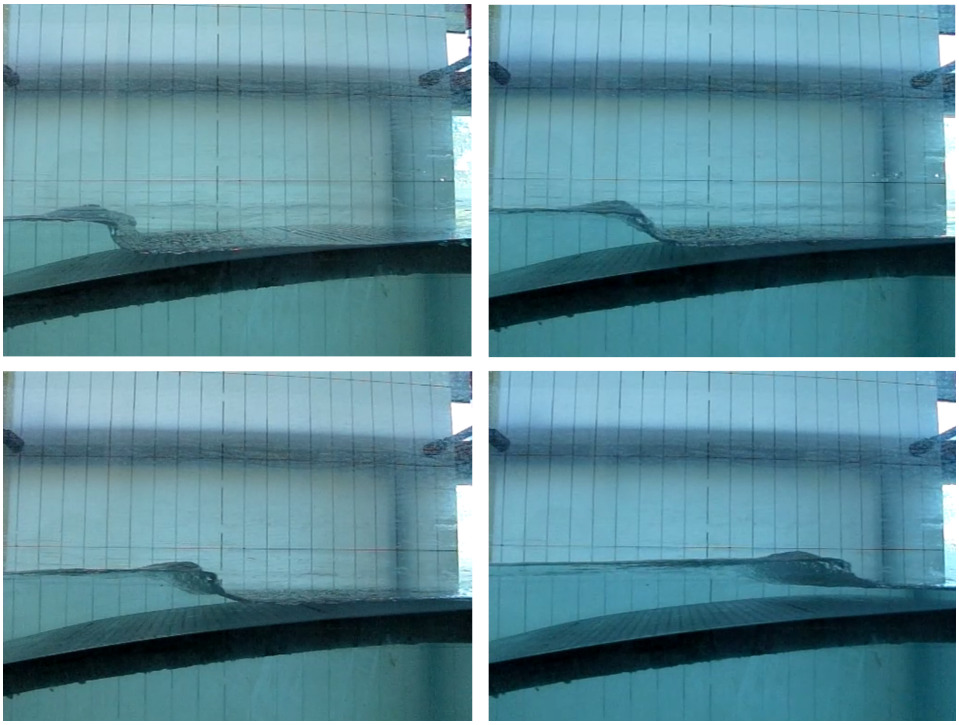

Figure 4.14: The approximate observed point of breaking for waves with full scale wave period of 12 seconds and steepness 1/60 for four different beach heights. Upper left: Top of beach at z = 0.01. Upper right: Top of beach at z = 0.00. Lower left: Top of beach at z = -0.01. Lower right: Top of beach at z = -0.025.

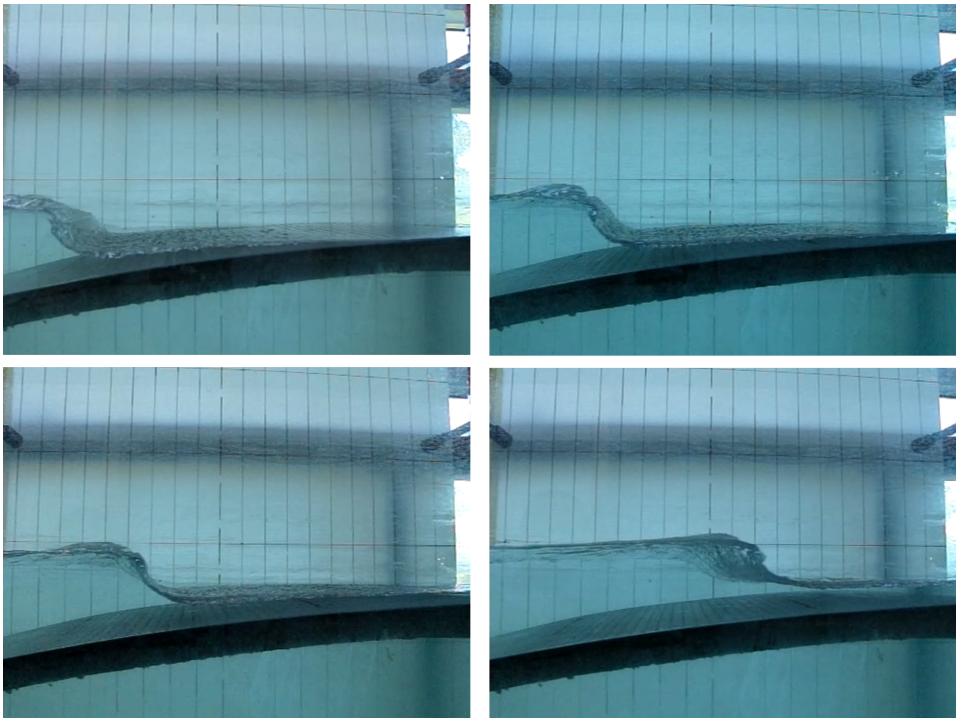

Figure 4.15: The approximate observed point of breaking for waves with full scale wave period of 12 seconds and steepness 1/45 for four different beach heights. Upper left: Top of beach at z = 0.01. Upper right: Top of beach at z = 0.00. Lower left: Top of beach at z = -0.01. Lower right: Top of beach at z = -0.025.

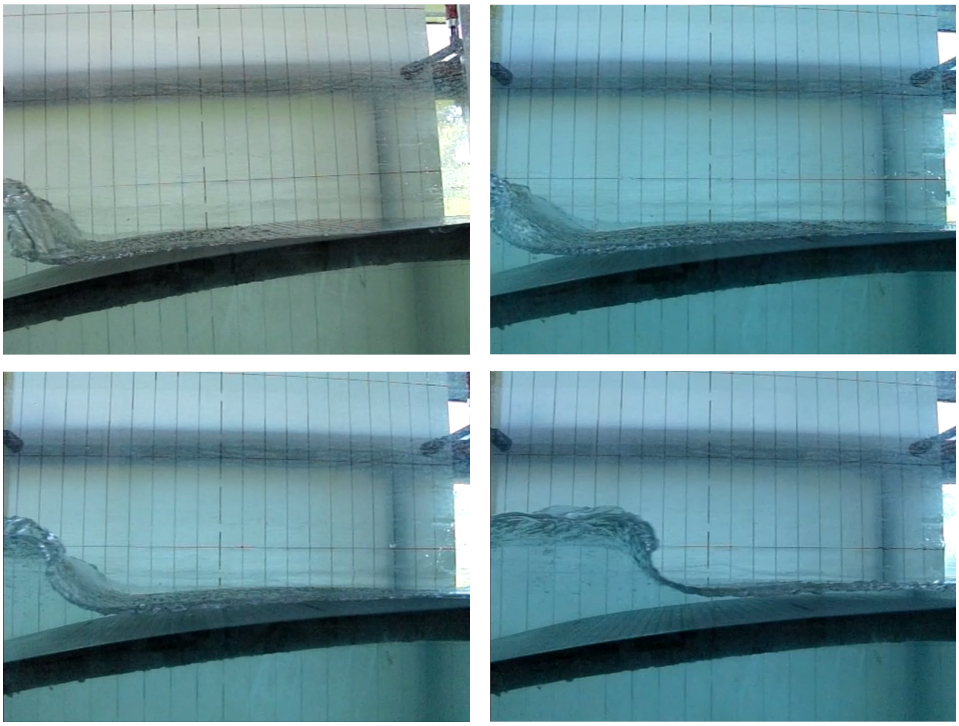

Figure 4.16: The approximate observed point of breaking for waves with full scale wave period of 12 seconds and steepness 1/30 for four different beach heights. Upper left: Top of beach at z = 0.01. Upper right: Top of beach at z = 0.00. Lower left: Top of beach at z = -0.01. Lower right: Top of beach at z = -0.025.

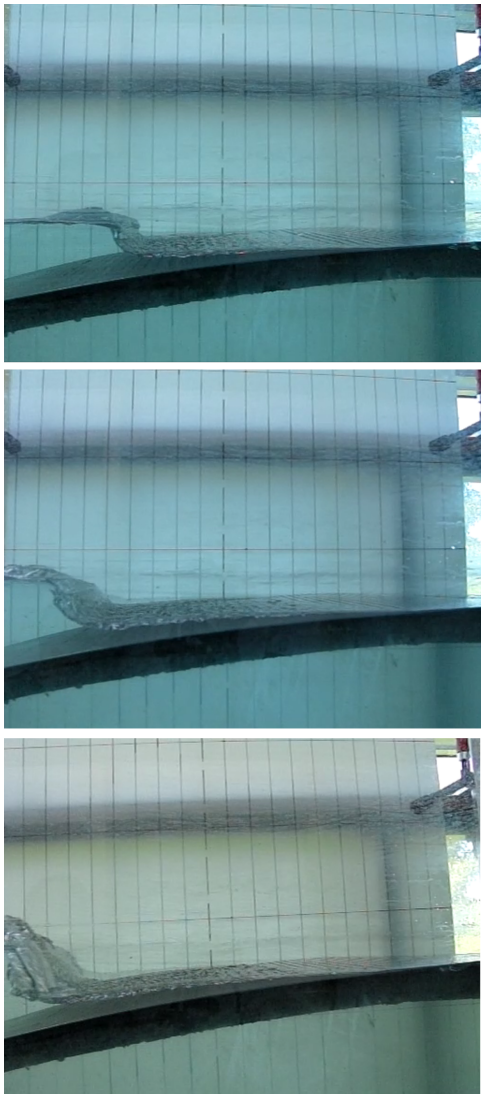

Figure 4.17: Comparison of observed point of breaking for waves with full scale wave period of 12 seconds and with top of beach at z = 0.01 for three different steepnesses. From the top and down: s = 1/60, s = 1/45 and s = 1/30.

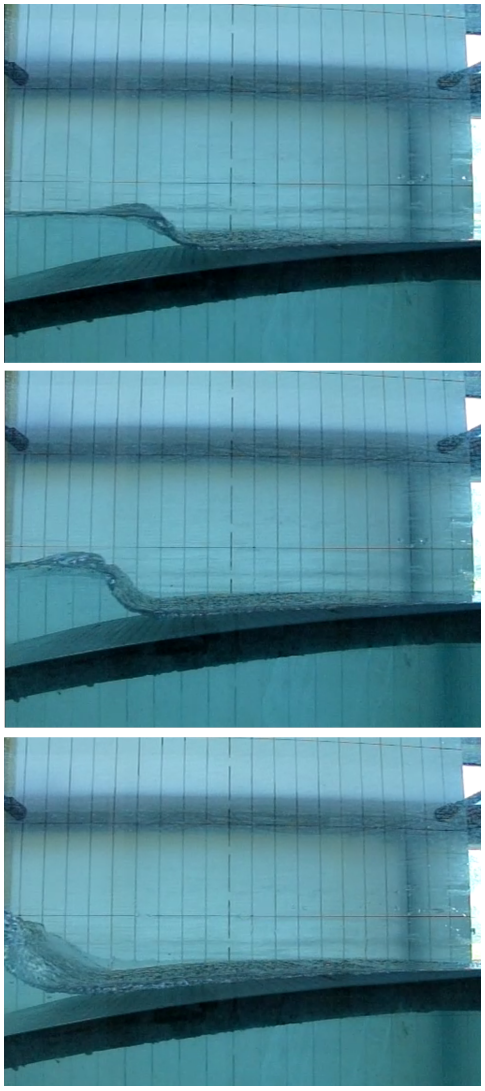

Figure 4.18: Comparison of observed point of breaking for waves with full scale wave period of 12 seconds and with top of beach at z = 0.00 for three different steepnesses. From the top and down: s = 1/60, s = 1/45 and s = 1/30.

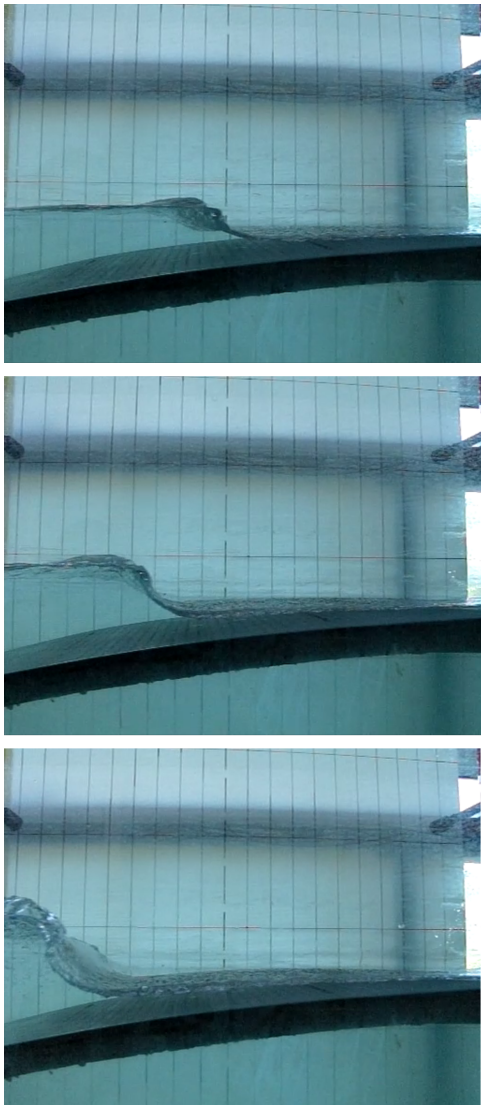

Figure 4.19: Comparison of observed point of breaking for waves with full scale wave period of 12 seconds and with top of beach at z = -0.01 for three different steepnesses. From the top and down: s = 1/60, s = 1/45 and s = 1/30.

Figure 4.20: Comparison of observed point of breaking for waves with full scale wave period of 12 seconds and with top of beach at z = -0.025 for three different steepnesses. From the top and down: s = 1/60, s = 1/45 and s = 1/30.

By defining the origin in a local coordinate system with x = 0 at the dashed line of the calibration plate and y = 0 by the beach surface, an approximated point of breaking can be found from the calibration plate. The rectangles on the calibration plate is 5 cm x 20 cm. The exact point of breaking was difficult to determine, even

with a high speed camera. The results are given in Table 4.8.

Beach top position	s = 1/60	s = 1/45	s = 1/30
z = 0.01	-200 mm	-300 mm	-400 mm
z = 0.00	-150 mm	-250 mm	-375 mm
z = -0.01	-100 mm	-175 mm	-300 mm
z = -0.025	100 mm	0 mm	-150 mm

Table 4.8: Approximated x-coordinates for point of observed breaking.

For which wave period the waves started breaking was also determined for four beach positions and all wave steepnesses and are found in Table 4.9

Beach top position	s = 1/60	s = 1/45	s = 1/30
z = 0.01	T = 7 s	T = 6 s	T = 5 s
z = 0.00	T = 7-8 s	T = 7 s	T = 6 s
z = -0.01	T = 8 s	T = 7-8 s	T = 6 s
z = -0.025	T = 9-10 s	T = 8-9 s	T = 7-8 s

Table 4.9: Approximated full scale wave period for point of observed breaking.

CHAPTER 5

Results

Results for experiments number one and three, and some for experiment two will be presented in this chapter. Experiment number two is rather large, and results should include many figures to justify the collected data. The main results from this experiment are therefore presented here, while the remaining plots can be found in the appendix.

5.1 Comparison Between Perforated and Non-Perforated Beach

This section consists of the results from the comparative study of the non-perforated and perforated beach in the Lader Wave Laboratory, experiment number one. Here the reflection coefficients are plotted as a function of the wave periods. Results for all wave conditions for the three beach positions will be presented. Only the least square method was used in this experiment.

Figure 5.1 shows the reflection coefficients for the non-perforated beach for the highest beach position in this experiment (z = 0.02). A clear trend can be seen with lower reflection coefficients for smaller waves and higher reflection coefficients for larger waves. However, the lowest reflection coefficients for waves with s = 1/60

and s = 1/45 are observed for waves with T = 1.14 s. For the shortest waves, the reflection coefficient is highest for the steepest waves and lower for less steep waves, opposite compared to the other wave periods. Despite the trend of gradually increasing K-values for higher wave periods, deviations are observed for waves with T = 1.14 s and shorter. The highest K-value is observed for the largest waves with the lowest steepness (12.05 %).

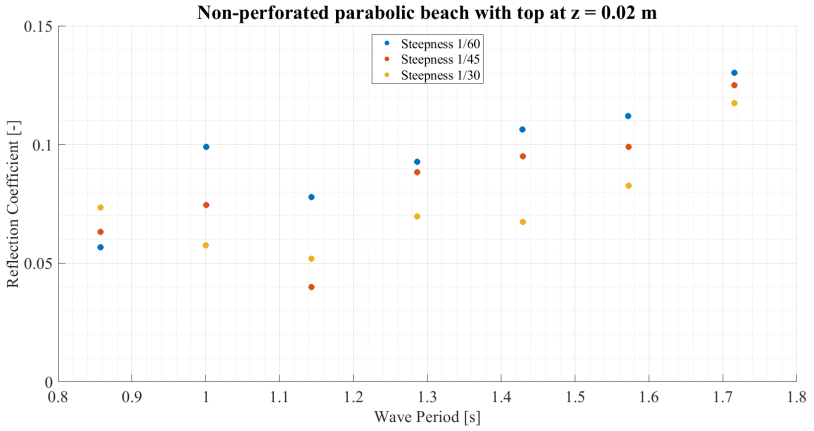

Figure 5.1: The reflection coefficient calculated using the least squares method plotted as a function of wave period for the non-perforated beach with top at z = 0.02.

The reflection coefficients for the perforated beach for the same height under the same wave conditions is shown in Figure 5.2. A similar trend as the non-perforated beach is observed with increasing K-values for larger waves. The reflection coefficient is, however, decreasing by about 60 % from T = 1.14 s to T = 1.29 s before increasing again. Another difference is that the steeper waves seem to lead to higher K-values than less steep waves for waves with T $<$1.43 while the opposite is the case for T $>$ 1.43. The reflection coefficients are significantly lower for all waves using the perforated beach compared to the non-perforated beach. The highest K-value is again observed for the largest waves with s = 1/60 (9.2 %) while the lowest is observed for T = 1.29 s, s = 1/60 ($>$ 1 %).

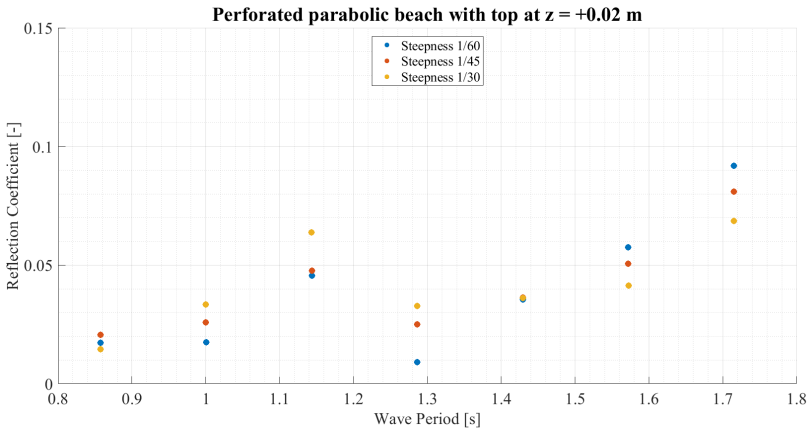

Figure 5.2: The reflection coefficient calculated using the least squares method plotted as a function of wave period for the perforated beach with top at z = 0.02.

The reflection coefficients calculated for the non-perforated when lowering the beach top to z = 0.00 can be seen in Figure 5.3. Here a similar trend as the highest beach position is observed for the waves with s = 1/30, but for waves with s = 1/60 and especially s = 1/45 the K-values are more constant for a large number of wave periods. This results in low reflection coefficients for the steepest waves in the mid-range of wave periods and higher reflection coefficients for the larger waves compared to the other steepnesses which is opposite of what was observed for the highest beach position. Also, an increase in K-values are seen for T = 1.14 s, and the highest K-value is observed at this wave period for s = 1/60 with K = 8.3 %.

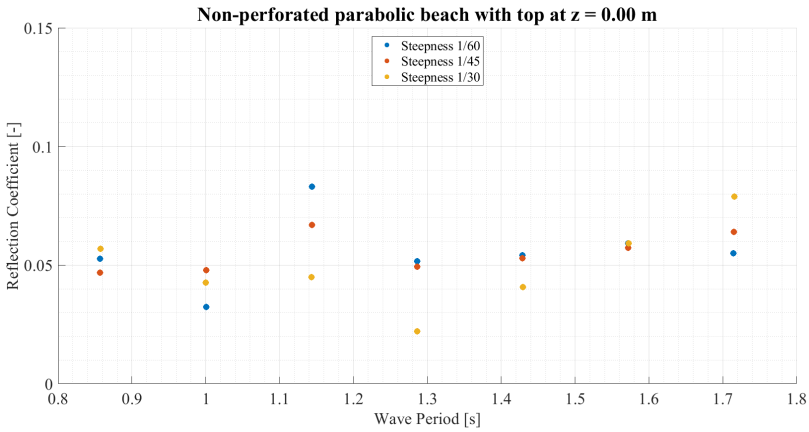

Figure 5.3: The reflection coefficient calculated using the least squares method plotted as a function of wave period for the non-perforated beach with top at z = 0.00.

Figure 5.4 shows the reflection coefficients for the perforated beach with the top of the beach at z = 0.00. This is the same beach height as the previous plot. For the perforated beach, the K-values are generally lower compared to the non-perforated beach, but the difference is not as significant as for the highest beach positions. Further, the shape is almost identical to the highest beach position for the same beach, except the reflection coefficients are lower. The largest K-value is 8.2 % compared to 9.2 % at z = 0.02.

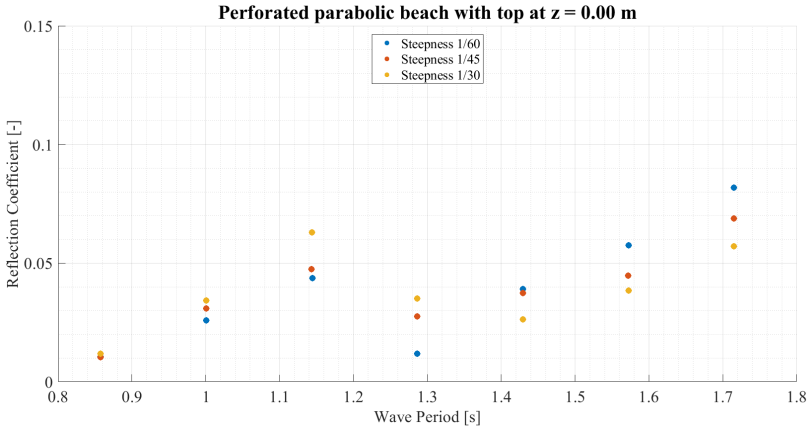

Figure 5.4: The reflection coefficient calculated using the least squares method plotted as a function of wave period for the perforated beach with top at z = 0.00.

Figures 5.5 and 5.6 shows the reflection coefficients for the lowest beach position (z = -0.02), for the non-perforated beach and the perforated beach respectively. The least reflected waves are observed for this beach height with K-values under 1 % for both beaches. The mean K-values were very similar, at 3.58 % for the non-perforated beach and 5.53 % for the perforated beach. For wave periods smaller than 1.3 s, the lowest reflection coefficients for the steepest waves were observed for the non-perforated beach, while for the least steep waves, the lowest K-values were observed for the perforated beach. For wave period longer than 1.3 s the opposite was observed.

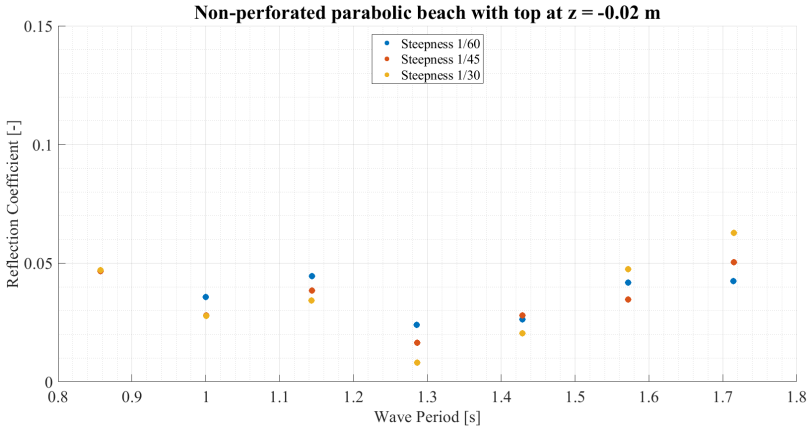

Figure 5.5: The reflection coefficient calculated using the least squares method plotted as a function of wave period for the non-perforated beach with top at z = -0.02.

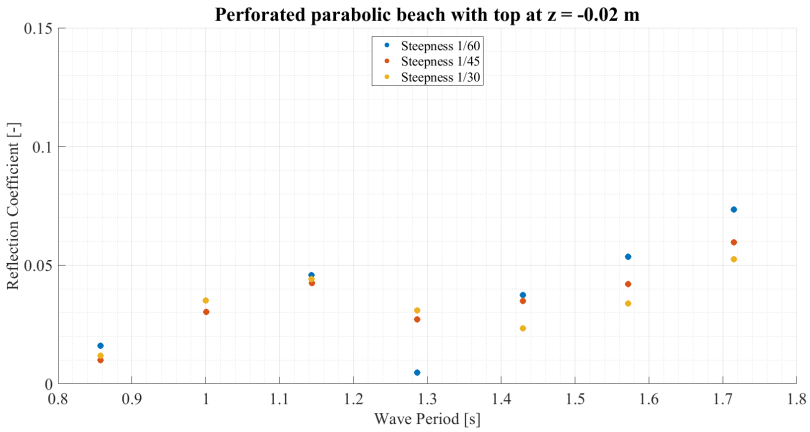

Figure 5.6: The reflection coefficient calculated using the least squares method plotted as a function of wave period for the perforated beach with top at z = -0.02.

Table 5.1 shows the mean reflection coefficient for the three beach positions for both beaches. The highest beach position seems to be the least efficient for both beaches for all wave steepnesses. The difference in beach position is most noticeable for the non-perforated beach, with a reflection coefficient 2.58 times higher compared to the perforated beach for waves with s = 1/60, but almost identical K-values for the lowest beach position. Further the table suggests that both beaches are more effective for steeper waves, except for the perforated beach when using the highest beach position.

Beach type and height	1/60	1/45	1/30
Non-perf. z = 0.02	9.64 %	8.35 %	7.43 %
Non-perf. z = 0.00	5.55 %	5.50 %	4.93 %
Non-perf. z = -0.02	3.74 %	3.47 %	3.54 %
Perforated z = 0.02	3.92 %	4.10 %	4.15 %
Perforated z = 0.00	3.86 %	3.82 %	3.80 %
Perforated z = -0.02	3.73 %	3.52 %	3.31 %

Table 5.1: Mean reflection coefficient calculated for all beach heights and wave steepnesses for both non-perforated and perforated beach using the least squares method.

5.2 Wave Reflection from Perforated Beach

This section consists of the results from experiment number two. The reflection coefficients are plotted as a function of wavelength divided by beach length, where the beach length is defined as the distance from the x-coordinate at the beach end closest to the wavemaker to the x-coordinate at the highest point of the beach. Wavelength divided by beach length can be written L_W/L_B. Both the least squares method results and the Goda's method results will be presented here.

Least Squares Method

Figure 5.7 is a scatter plot of the Reflection coefficients for the highest beach position (z = 0.025 m) in experiment two using the least square method. Observe that there is a large range of calculated values for the reflection coefficients for waves with a wavelength shorter than the defined beach length of 1.80 meters. The smallest waves, close to half the beach length and shorter seems to have the most spreading. Three measurements were recorded with a reflection coefficient higher than 0.15, with K = 0.191, 0.195 and 0.248, all for the same wavelength of 0.88 meters. For waves with wavelengths longer than the beach length, there was less spreading of the calculated reflection coefficients and the trends become visible. For waves with wavelengths ranging from 1 to 1.5 times the beach length, the reflection coefficient seems to be more or less constant with some deviations. The reflection of the longest waves, over 1.5 times the beach length, is more consistent. Here a clear trend can be seen with strictly increasing K-values for increasing wavelength for the waves with both steepness 1/60 and 1/45. The waves with s = 1/30 are almost strictly increasing as well. Further, the waves with a steepness of 1/60 seem to have the highest reflection coefficients and steeper waves lead to lower reflection coefficients.

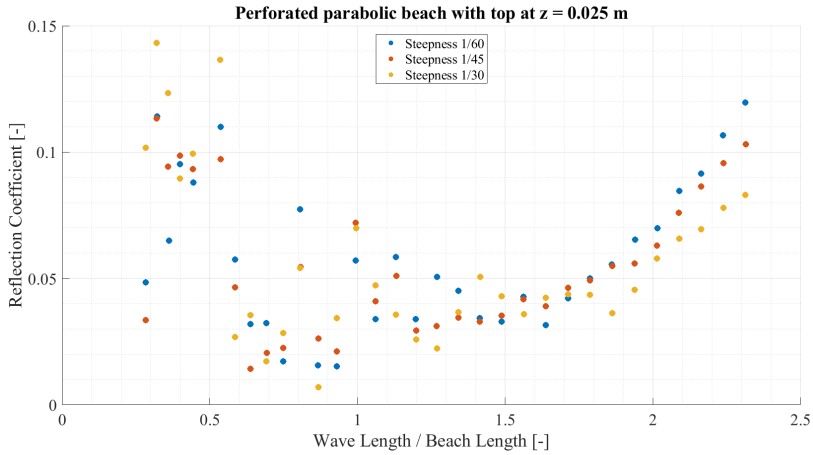

Figure 5.7: The reflection coefficient calculated using the least squares method plotted as a function of wavelength divided by beach length for beach with top at z = 0.025.

In Figure 5.8, a scatter plot from the same experiment is shown with the same wave conditions. The only difference is the beach position with the top of the beach submerged to z = -0.025 (the lowest position in this experiment). Similar results are found for both the highest and lowest beach position. The shortest waves are again the waves with the highest K-values, and the values are varying a lot from one wave condition to another. For wavelengths larger than the beach length the reflection coefficient is gradually increasing to 5 % for wavelengths up to 1.5 times the beach length. Further, there is a decrease to about 3 % at 1.75 times the beach length. From there, K-values are almost strictly increasing for all steepnesses.

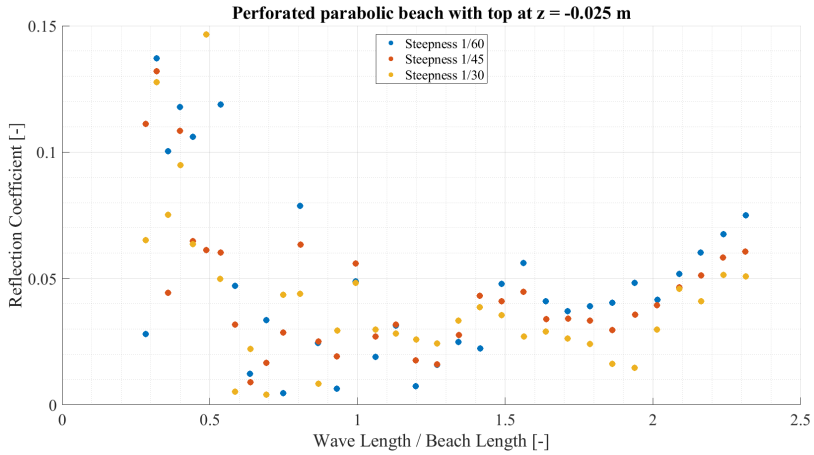

Figure 5.8: The reflection coefficient calculated using the least squares method plotted as a function of wavelength divided by beach length for beach with top at z = -0.025.

By looking at the reflection coefficients for waves with $L_W/L_B > 1$, it is evident that they are smaller for the lower beach position, suggesting that this might be a more effective position for larger waves. Another important difference between the two plots is that for wavelengths larger than the beach length, the upper beach position seems to be equally efficient in the range $1.2 < L_W/L_B < 1.7$. In the lower position, however, it looks like the K-values approach a local minimum at both $L_W/L_B = 1.2$ and $L_W/L_B = 1.75$ with a distinct local maximum at around $L_W/L_B = 1.5$. Thus making the slope different for the two beach positions.

In Figure 5.9 a third-degree polynomial curve fit is used to compare the reflection coefficients for the different beach positions. Only waves longer than the beach length and waves with steepness 1/30 is considered in these plots. Here the results from comparison of the two previous figures (5.7 and 5.8) can be recognised. The higher beach position is the least effective for the longest waves, while the lower beach positions seem to be the most effective. It can also be seen that the reflection coefficient is gradually decreasing with lower beach positions for all five positions when $L_W/L_B > 1.65$. Interestingly, the second lowest beach position has the straightest curve fit, while the lowest beach position leads to the most curved line.

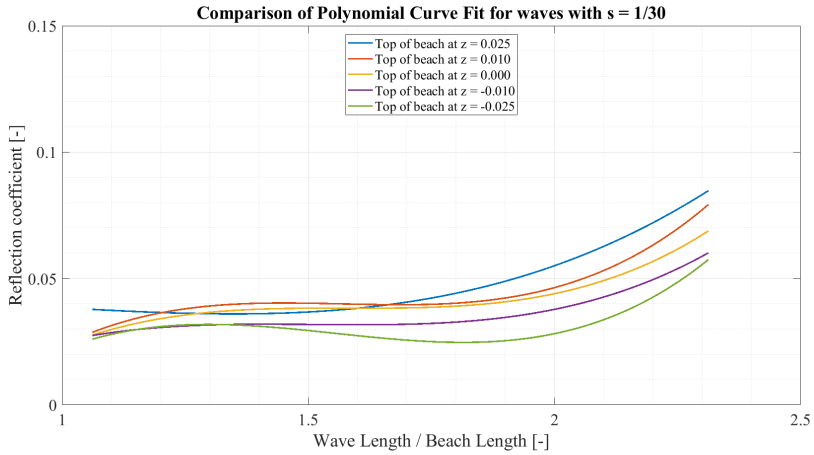

Figure 5.9: Comparison of reflection coefficients by using third degree polynomial curve fit for all five beach positions. Only waves longer than the beach length are included and only the steepest waves with s = 1/30.

Table 5.2 shows the mean calculated reflection coefficients for each beach position for every wave steepness using the least squares method. Here it can be seen what was also shown in Figure 5.9, that the beach efficiency increases with steeper waves and lower beach position.

Beach height	Reflection all steepnesses	1/60	1/45	1/30
z = 0.025	5.33 %	5.83 %	5.37 %	4.79 %
z = 0.010	4.98 %	5.45 %	5.02 %	4.48 %
z = 0.000	4.76 %	5.26 %	4.82 %	4.19 %
z = -0.010	4.23 %	4.82 %	4.25 %	3.62 %
z = -0.025	3.65 %	4.04 %	3.73 %	3.18 %

Table 5.2: Mean reflection coefficient calculated for waves longer than the beach length for all beach heights and wave steepnesses using the least squares method.

Goda's Method

This subsection consists of plots of the same beach positions and wave conditions as for the least squares method, only this time using Goda's method. Remember that Goda's method is inaccurate when the probe spacing is equal to an integer number of half wavelengths. Wave probes 1 and 2 were used in the calculations, and the waves with a wavelength between 40 % and 60 % of the probe spacing are

therefore excluded from these plots.

Figure 5.10 shows the reflection coefficients calculated for the highest beach position (z = 0.025). The overall results are very similar to the reflection coefficients calculated using the least squares method. Notice the K-values that are filtered out at $L_W/L_B \approx 0.5 - 0.6$ due to the wave probe spacing being close to half of their wavelengths. For waves shorter than half of the beach length the K-values are deviating a lot with quantities ranging from 5.7 % to 19.0 %. Deviations are also large for $0.5 < L_W/L_B < 1.0$ where the K-values are varying a lot for small changes in wavelengths. For waves longer than the beach length more consistent trends are observed with gradually increasing reflection coefficients for larger waves. The beach seems again most efficient for the steepest waves and least efficient for waves with s = 1/60.

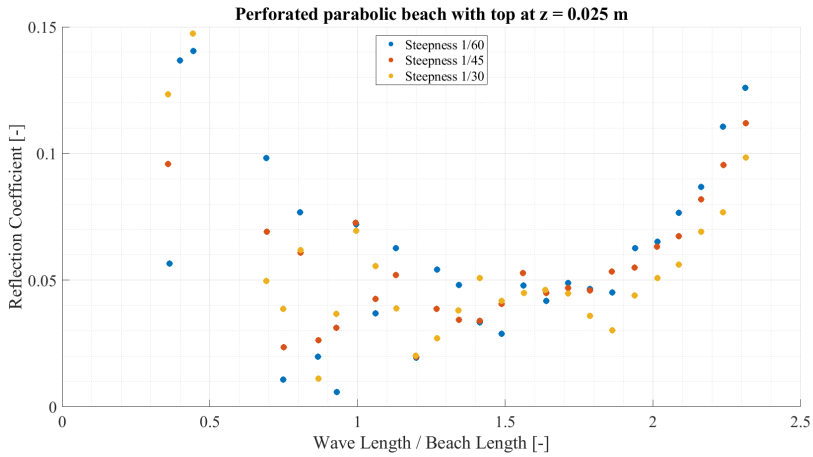

Figure 5.10: The reflection coefficient calculated using Goda's method plotted as a function of wavelength divided by beach length for beach with top at z = 0.025.

In Figure 5.11 the reflection coefficients calculated for the lowest beach position (z = -0.025) is shown. Again the results using Goda's method are very similar to the results from the least square method calculations for the same beach position. The K-values for waves shorter than half of the beach length are as inconsistent as previously with values between 5.1 % to 16.3 %. Reflection coefficients for waves with $0.5 < L_W/L_B < 1.0$ are also varying, from several measurements under 1 % up to 7.9 %. For the larger waves ($L_W/L_B > 1.0$) the K-values are following the same trend as described using the least squares method where they are gradually increasing for wavelengths up to 1.5 times the beach length, then decreasing before increasing again for $L_W/L_B > 1.9$. Again the beach efficiency

is higher for steeper waves.

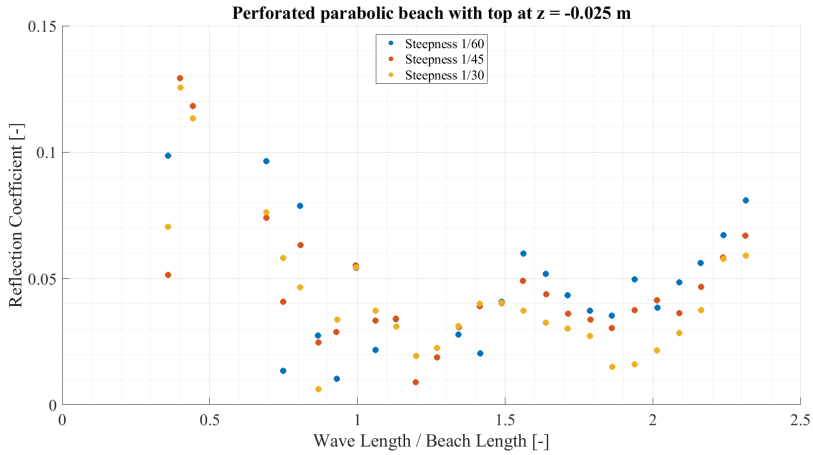

Figure 5.11: The reflection coefficient calculated using Goda's method plotted as a function of wavelength divided by beach length for beach with top at z = -0.025.

Figure 5.12 shows a third-degree polynomial curve fit for each beach position using Goda's method. The polynomial is calculated only using the K-values for waves longer than the beach length with s = 1/30 (similar to Figure 5.9). The plots give similar results for all beach positions for both methods. The reflection coefficients are slightly lower for calculations done using Goda's method which is also seen when comparing Tables 5.2 and 5.3. It is also observed that the curve fits are a bit more s-shaped using Goda's method, especially for z = -0.010.

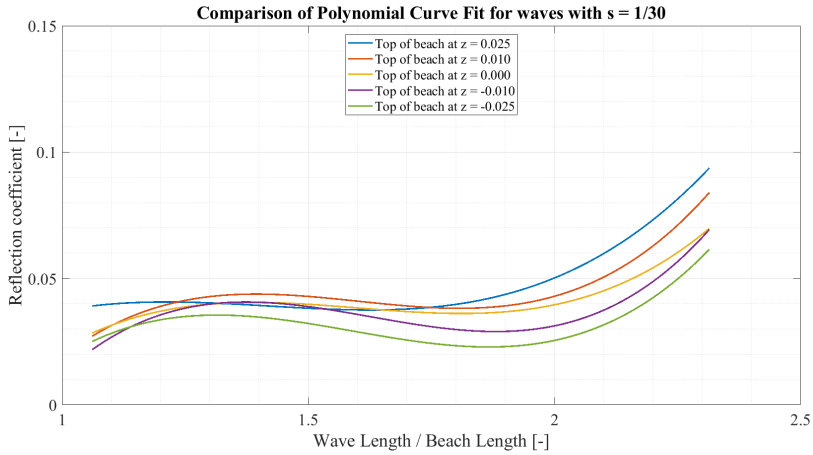

Figure 5.12: Comparison of reflection coefficients by using third degree polynomial curve fit for all five beach positions. Only waves longer than the beach length are included and only the steepest waves with s = 1/30.

Beach height	Reflection all steepnesses	1/60	1/45	1/30
z = 0.025	5.35 %	5.78 %	5.45 %	4.83 %
z = 0.010	5.00 %	5.47 %	5.00 %	4.53 %
z = 0.000	4.73 %	5.19 %	4.86 %	4.14 %
z = -0.010	4.23 %	4.78 %	4.17 %	3.75 %
z = -0.025	3.72 %	4.11 %	3.81 %	3.24 %

Table 5.3: Mean reflection coefficient calculated for waves longer than the beach length for all beach heights and wave steepnesses using Goda's method.

5.3 Wave Reflection in Shallow Water

This section describes the results from experiment number three, done in the small towing tank with finite water conditions. Only one beach position was tested in this experiment with the top of the beach at z = 0.01. The K-values are here plotted as a function of wavelength divided by beach length. The beach length is defined similarly to the beaches in the Lader Wave Laboratory, the distance of the x-position of the end nearest the wavemaker to the x-position of the highest point of the beach, 2.70 meters. The wave periods used in this experiments corresponds to full-scale wave periods ranging from 4 seconds to 15 seconds with 0.5 seconds increments.

In Figure 5.13, a scatter plot is shown of the calculated reflection coefficients using the least squares method for wave probes 2A, 3A and 4A. A trend of increasing K-values is observed for increasing wavelengths when considering all wavelengths. However, the reflection coefficients are increasing and decreasing in intervals. For $0.3 < L_W/L_B < 0.6$ a local maximum is observed for $L_W/L_B \approx 0.4$. Similarly for $0.7 < L_W/L_B < 1.1$, $1.1 < L_W/L_B < 1.4$ and $L_W/L_B > 1.4$ with local maximums at $L_W/L_B \approx 0.9$, $L_W/L_B \approx 1.3$ and $L_W/L_B \approx 1.6$. This trend is observed for all wave steepnesses and is not found for the experiments done in the Lader Wave Laboratory with greater water depth. In this experiment, the beach efficiency was highest for the steeper waves for most wavelengths, both shorter and longer waves. The reason for the point in (0,0) is that the first wave period corresponding to 4 seconds in full scale failed because of wave probes being positioned too far away from the beach.

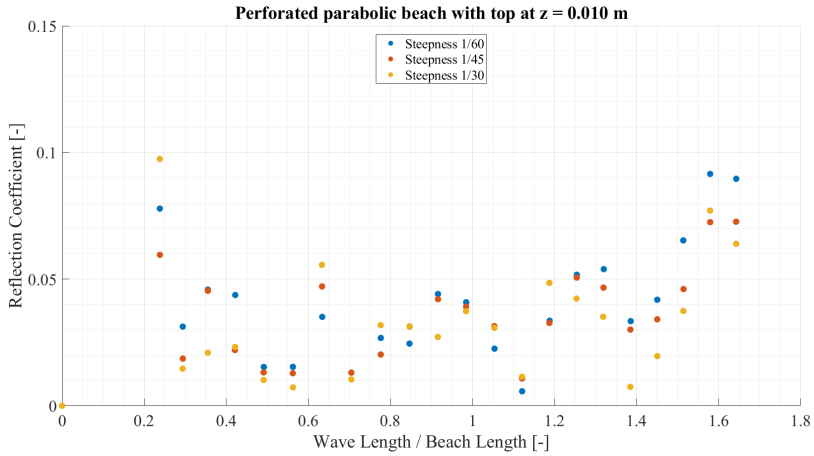

Figure 5.13: The reflection coefficient calculated using the least squares method plotted as a function of wavelength divided by beach length for perforated beach in the small towing tank with top at z = 0.01.

CHAPTER 6

Discussion

Calculated Reflection Coefficients

Starting with experiment number two, calculation of reflection coefficients larger than the beach length resulted in very similar results using both the least squares method and Goda's method. This indicates that the calculated K-values are most likely close to the physical reflection coefficients. A clear and consistent trend of increasing K-values for all wavelengths is shown in multiple plots for different experiments. The problems occur for wavelengths shorter than the beach length where results are inconsistent when comparing the two methods. The magnitude of wave reflection is still reasonable for the longer waves and comparable results are observed for similar experiments. One could argue that one of the methods or both fail for certain wavelengths because of the probe distance chosen during the set up of the experiment. The deviations are not as noticeable for experiments one (with longer probe spacing) and experiment three (with shorter probe spacing). However, for experiment one, the same deviations should arguably occur for longer waves. Nevertheless, this is the reason why waves longer than the beach length were emphasized in experiment two. It is still unclear why both methods seem to fail for shorter waves.

Another interesting observation is the phenomenon of periodically increasing and

decreasing reflection coefficients over a short range of wavelengths. This was observed multiple times in experiment two, primarily for the lower beach positions, which led to a slightly s-shaped curve using a third-degree polynomial curve fit. The phenomenon is shown clearly in Figure 5.13 from experiment three under finite water conditions for all wave steepnesses. An explanation for this could be second-order parasitic waves. Parasitic waves are free waves that could be created by a wavemaker motion or breaking waves (near a beach). Parasitic waves are described in some detail by Kristiansen and Faltinsen [6]. The measurement series are filtered around the first harmonic, but the second-order parasitic waves influence the first and third harmonic, giving a contribution to the measured time series despite being filtered around the first harmonic.

To find more information about this, the theoretical and calculated incident waves were plotted together, see Figure 6.1. The theoretical wave amplitude is the amplitude calculated from the measured wavemaker amplitudes for the hinged flap wavemaker. The calculated incident wave amplitude is the incident amplitude calculated using the least squares method. This was done for wave periods corresponding to periods from 4 seconds to 12 seconds in full scale for all steepnesses. Notice that the calculated amplitude is lower than the theoretical amplitude. This can be explained partially with the wavemaker not covering the entire tank width. In fact, the wavemaker only covers about 97 % of the transverse area in the tank. Interestingly, similar deviations as described in context with parasitic waves are observed for the calculated incident waves for all steepnesses for the same wave periods.

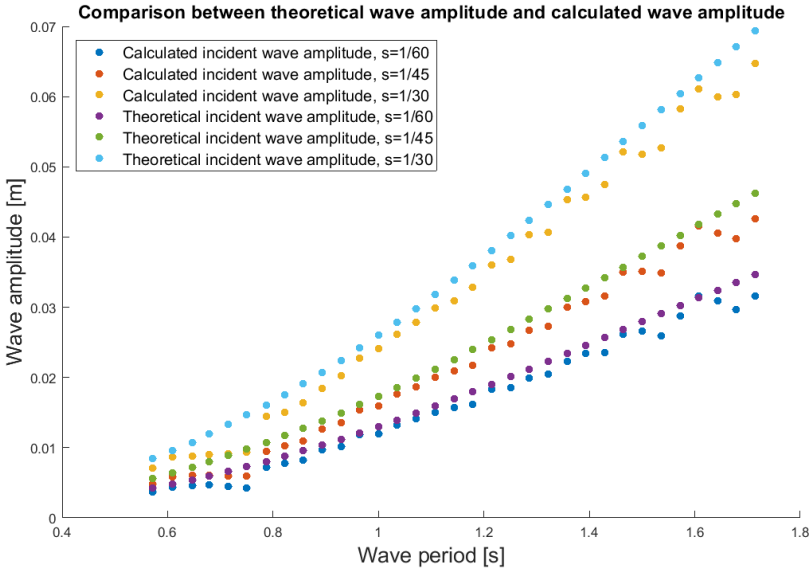

Figure 6.1: Comparison of the theoretical incident wave amplitude and the calculated incident wave amplitude using the least squares method for all three steepnesses.

In Figure 6.2, the theoretical incident wave amplitude is reduced by 3 % and is correlating well the calculated incident wave amplitude except for the periodical deviations discussed. The amplitudes of the reflected waves are also shown in this plot, and similar behaviour can be observed here. The reason for this is unknown. Notice the incident wave amplitude dropping around T = 5.5, while the reflected wave amplitude increases. This leads to a very large reflection coefficient of 25 %, which is considered unlikely. This suggests that the method fails in this area.

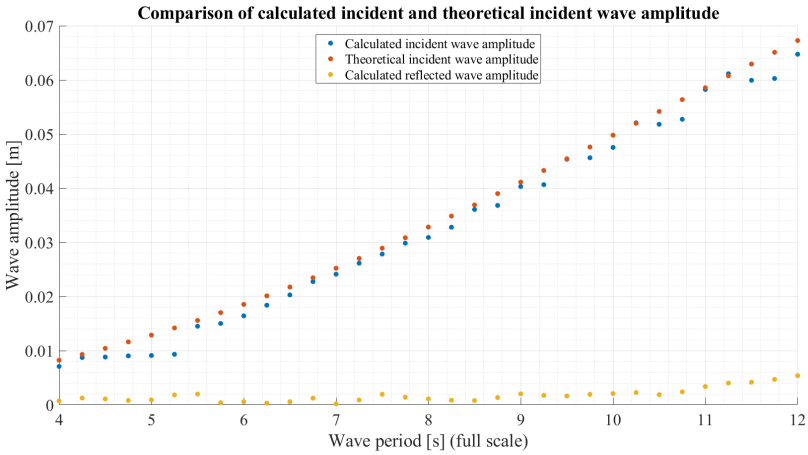

Figure 6.2: These are quantities calculated for waves with periods from 4 s to 12 s and steepness 1/30. The figure shows the comparison of the theoretical incident wave amplitude after correction and the calculated incident wave amplitude using the least squares method. The calculated reflected wave amplitudes using least squared method are also plotted.

CHAPTER 7

Conclusions

In experiment one, where the non-perforated beach was compared to the perforated beach, it was found that the perforated beach was overall more efficient, leading to 52.4 % lower reflection coefficients. The difference was greatest for the highest beach position (z = 0.02), where the mean reflection coefficient was 109 % higher for the non-perforated beach compared to the perforated beach. For the lower beach positions, the difference becomes less significant, and the perforated beach shows only 1.7 % higher efficiency.

The non-perforated beach was more efficient for steeper waves in all beach positions compared to the least steep waves with an average K-value of 0.53 for s = 1/30 and 0.63 for s = 1/60. The perforated beach was also more efficient for the steeper waves in the lowest beach position and slightly more efficient in the mid position (z = 0.00), but most efficient for the less steep waves in the highest beach position.

The purpose of experiment number two was to calculate the wave reflection from the perforated beach for a larger number of wave periods and beach heights. It was observed that the reflection coefficient was strictly decreasing with lower beach positions and steeper waves when considering the mean K-values for waves longer than the defined beach length. This is consistent with what was found in experiment one. The reflection coefficient was decreased by 46 % by lowering the beach

from z = 0.025 to z = -0.025 for waves longer than the beach length.

The reflection coefficients calculated using the least squares method and Goda's method were almost identical for all waves longer than the beach length, but large deviations were found for the shorter waves for all beach positions. Three calculations of reflection coefficients for the perforated beach with height z = 0.00 are done. The mean K-values for wavelengths larger than the beach length are 0.482 (experiment one), 0.476 (least squares, ex two) and 0.473 (Goda's, ex two) which is a good correspondence.

In experiment three, some of the same trends found in experiment one and two were observed in finite water conditions. The reflection coefficients are gradually increasing with wavelength, but with more noticeable local variations, which could be caused by parasitic waves.

Bibliography

[1] O. M. Faltinsen. *Sea Loads on Ships and Offshore Structures*. Cambridge Ocean Technology. Cambridge University Press, 1990.

[2] Robert G. Dean and Robert A. Darymple. Water wave mechanics for engineers and scientists, 1984. Advanced Series on Ocean Engineering - Volume 2.

[3] E P D Mansard and E R Funke. The measurement of incident and reflected spectra using a least squares method. 03 1980.

[4] Yoshimi Goda and Yasumasa Suzuki. *Estimation of Incident and Reflected Waves in Random Wave Experiments*, pages 828–845.

[5] Michael Isaacson. Measurement of regular wave reflection. *Journal of Waterway, Port, Coastal, and Ocean Engineering*, 117(6):553–569, 1991.

[6] T. Kristiansen and O. M. Faltinsen. Higher harmonic wave loads on a vertical cylinder in finite water depth. *Journal of Fluid Mechanics*, 833:773–805, 2017.

APPENDIX A

Plots From Experiment Two

A.1 Reflection coefficients for the five beach positions using least squares method

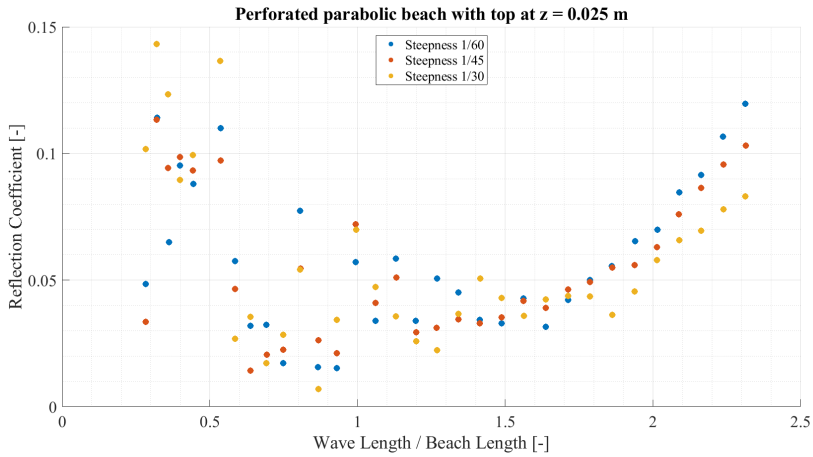

Figure A.1: The reflection coefficient calculated using the least squares method plotted as a function of wavelength over beach length for beach with top at z = 0.025.

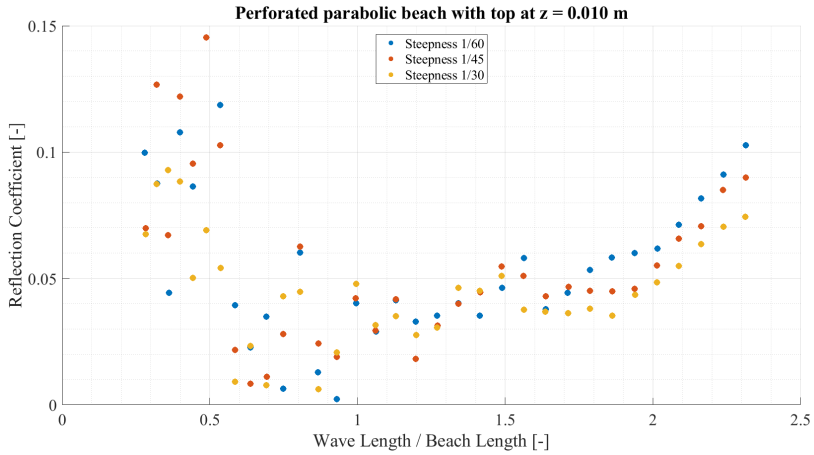

Figure A.2: The reflection coefficient calculated using the least squares method plotted as a function of wavelength over beach length for beach with top at z = 0.01.

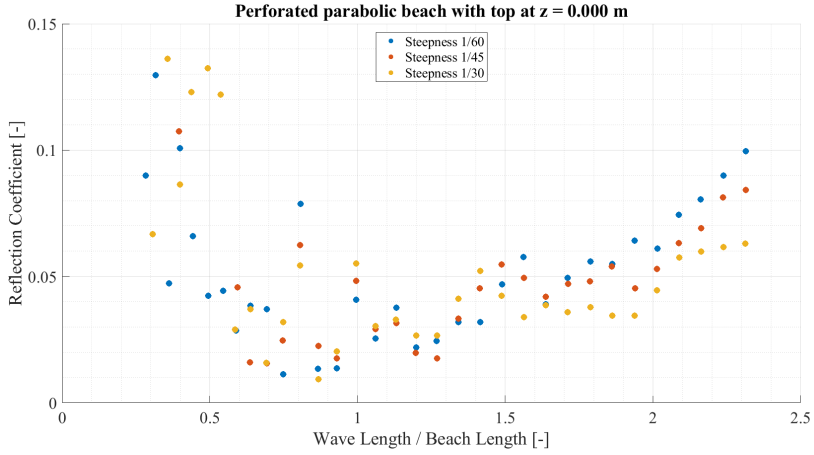

Figure A.3: The reflection coefficient calculated using the least squares method plotted as a function of wavelength over beach length for beach with top at z = 0.

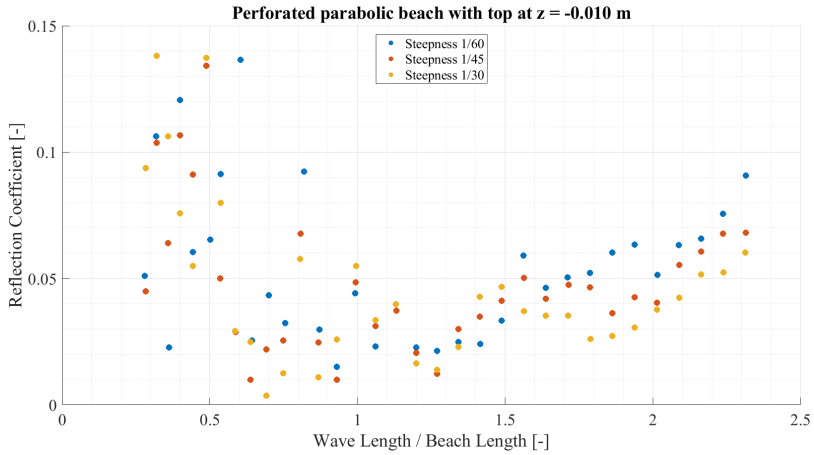

Figure A.4: The reflection coefficient calculated using the least squares method plotted as a function of wavelength over beach length for beach with top at z = -0.01.

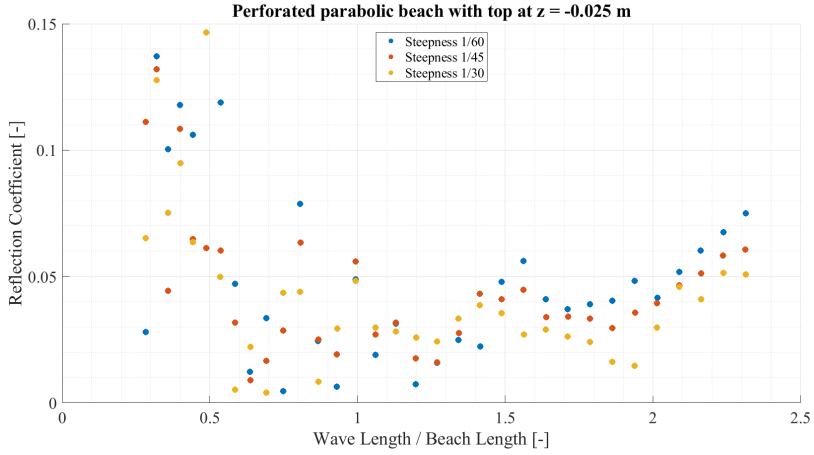

Figure A.5: The reflection coefficient calculated using the least squares method plotted as a function of wavelength over beach length for beach with top at z = -0.025.

A.2 Reflection coefficients for the five beach positions using Goda's method

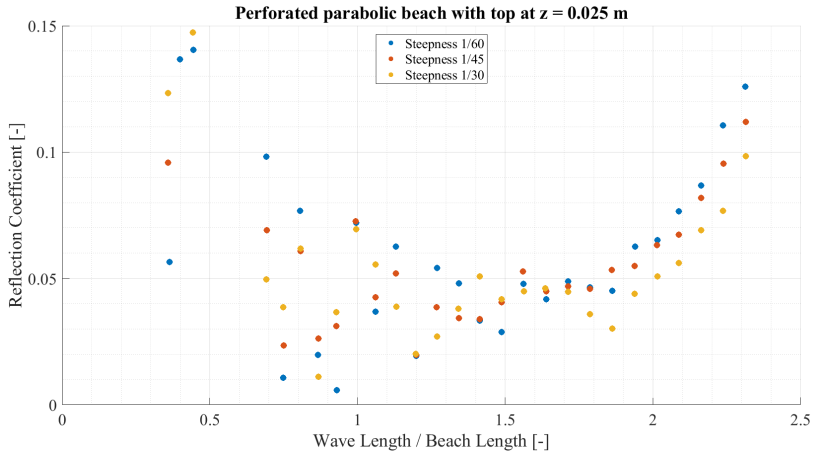

Figure A.6: The reflection coefficient calculated using the Goda's method plotted as a function of wavelength over beach length for beach with top at z = 0.025.

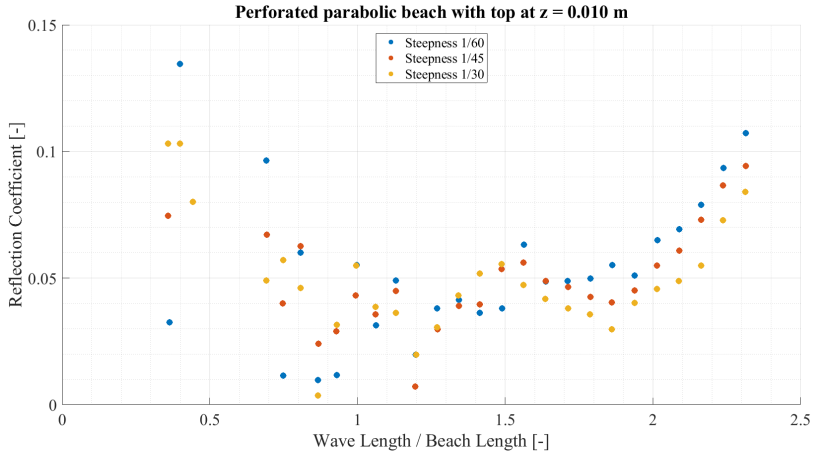

Figure A.7: The reflection coefficient calculated using the Goda's method plotted as a function of wavelength over beach length for beach with top at z = 0.01.

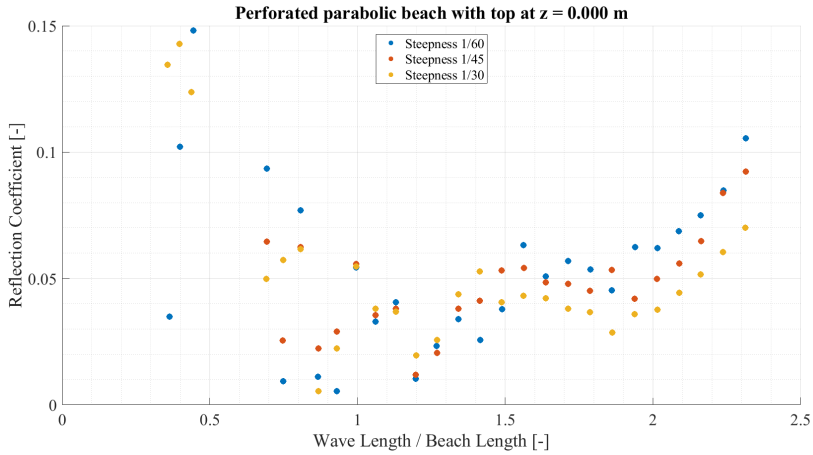

Figure A.8: The reflection coefficient calculated using the Goda's method plotted as a function of wavelength over beach length for beach with top at z = 0.

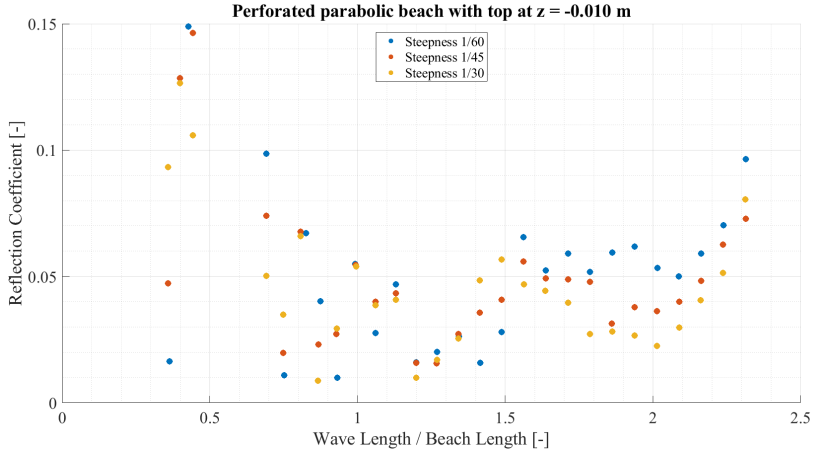

Figure A.9: The reflection coefficient calculated using the Goda's method plotted as a function of wavelength over beach length for beach with top at z = -0.01.

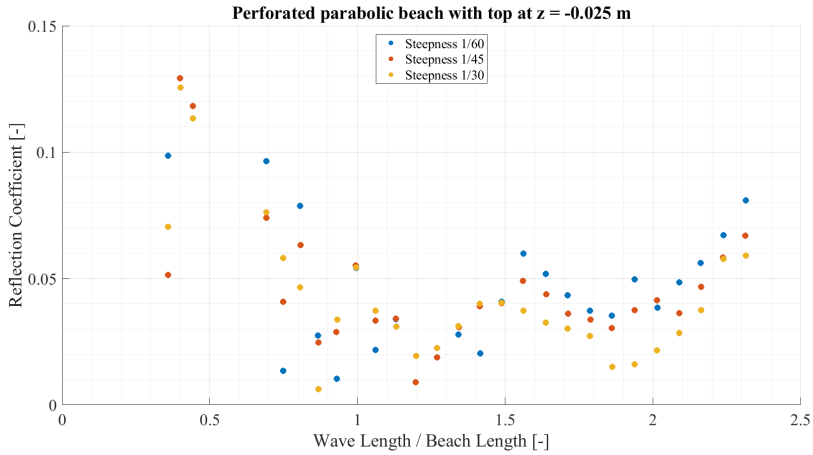

Figure A.10: The reflection coefficient calculated using the Goda's method plotted as a function of wavelength over beach length for beach with top at z = -0.025.

A.3 Polynomial curve fit for reflection coefficients for five beach positions using the least squares method

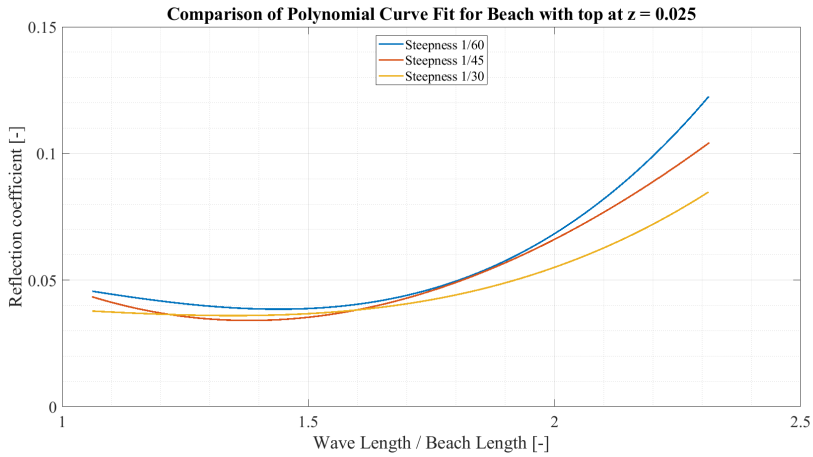

Figure A.11: Comparison of reflection coefficients by using third degree polynomial curve fit for all three wave steepnesses. Beach height is z = 0.025 and only waves longer than the beach length are included.

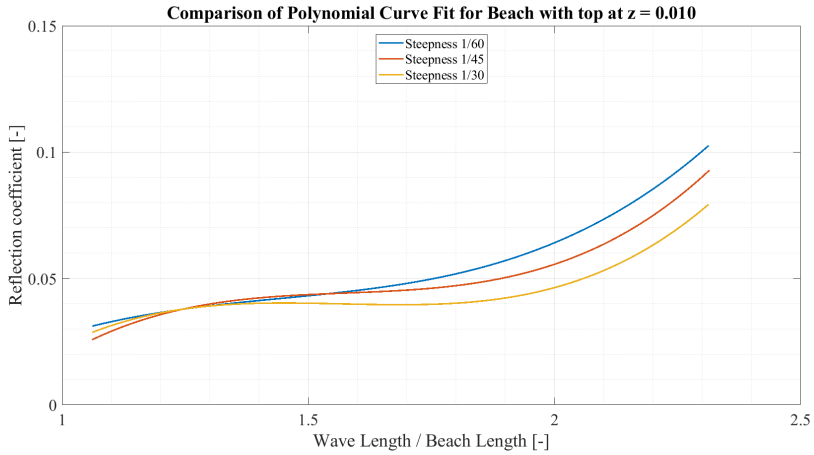

Figure A.12: Comparison of reflection coefficients by using third degree polynomial curve fit for all three wave steepnesses. Beach height is z = 0.01 and only waves longer than the beach length are included.

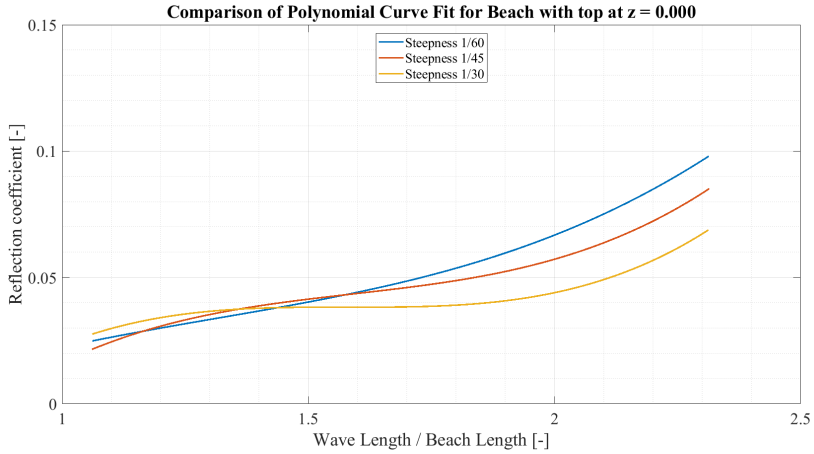

Figure A.13: Comparison of reflection coefficients by using third degree polynomial curve fit for all three wave steepnesses. Beach height is z = 0 and only waves longer than the beach length are included.

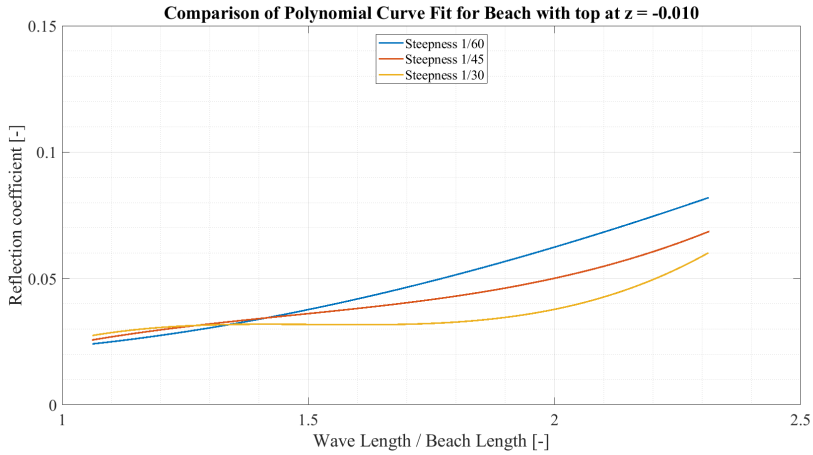

Figure A.14: Comparison of reflection coefficients by using third degree polynomial curve fit for all three wave steepnesses. Beach height is z = -0.01 and only waves longer than the beach length are included.

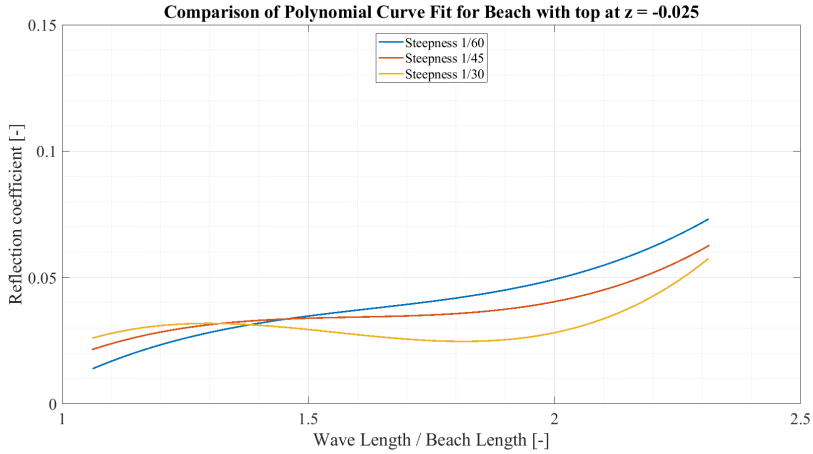

Figure A.15: Comparison of reflection coefficients calculated by using third degree polynomial curve fit for all three wave steepnesses. Beach height is z = -0.025 and only waves longer than the beach length are included.

A.4 Polynomial curve fit for reflection coefficients for five beach positions using Goda's method

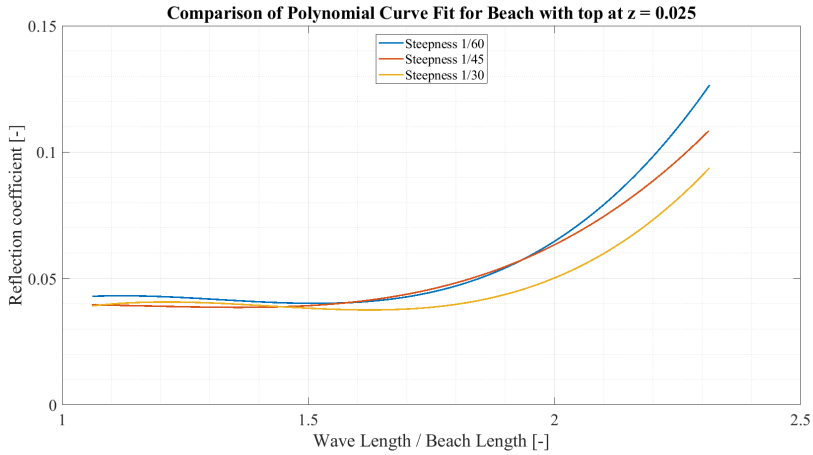

Figure A.16: Comparison of reflection coefficients by using third degree polynomial curve fit for all three wave steepnesses. Beach height is z = 0.025 and only waves longer than the beach length are included.

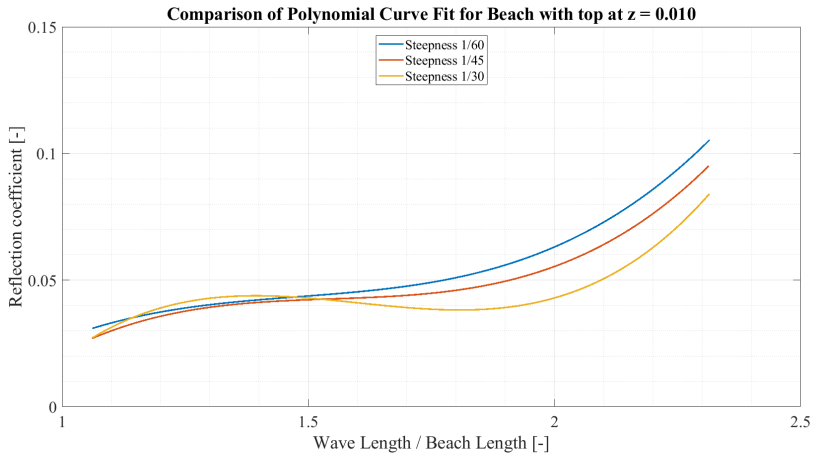

Figure A.17: Comparison of reflection coefficients by using third degree polynomial curve fit for all three wave steepnesses. Beach height is z = 0.01 and only waves longer than the beach length are included.

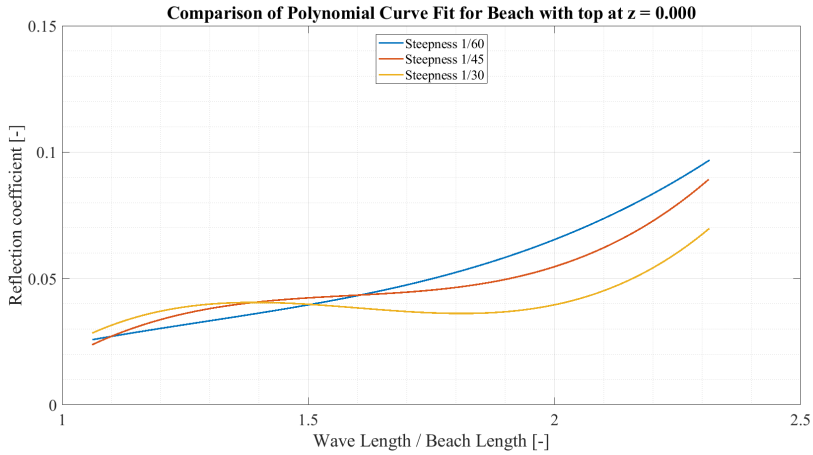

Figure A.18: Comparison of reflection coefficients by using third degree polynomial curve fit for all three wave steepnesses. Beach height is z = 0 and only waves longer than the beach length are included.

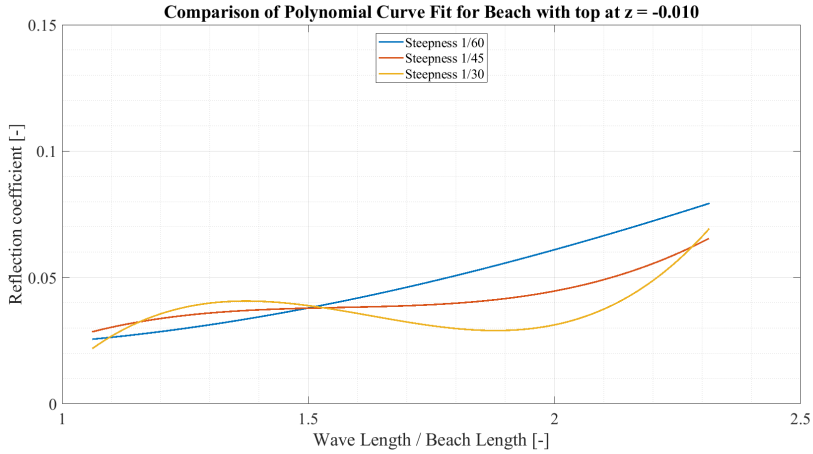

Figure A.19: Comparison of reflection coefficients by using third degree polynomial curve fit for all three wave steepnesses. Beach height is z = -0.01 and only waves longer than the beach length are included.

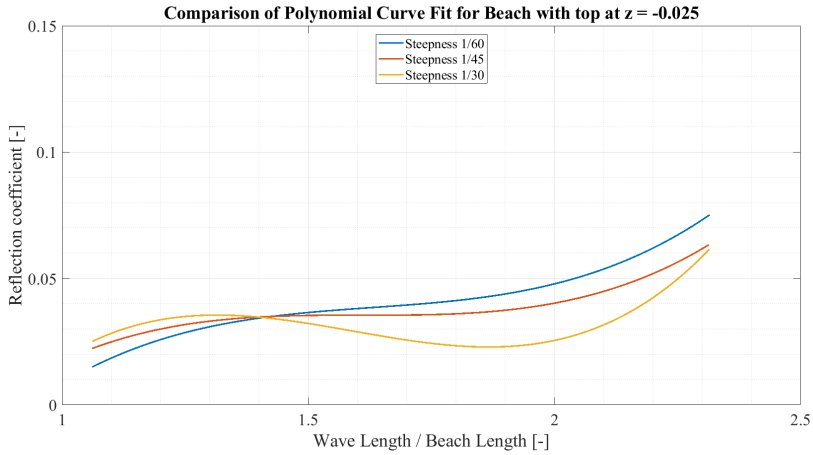

Figure A.20: Comparison of reflection coefficients calculated by using third degree polynomial curve fit for all three wave steepnesses. Beach height is z = -0.025 and only waves longer than the beach length are included.

A.5 Polynomial curve fit for reflection coefficients for three wave steepnesses using the least squares method

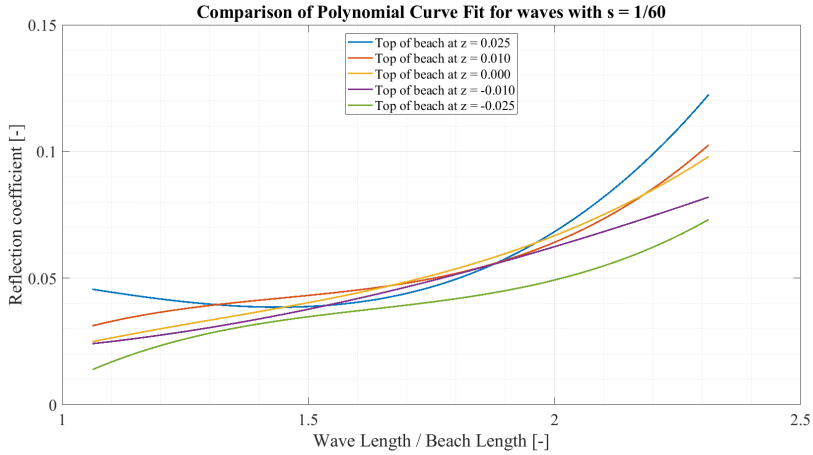

Figure A.21: Comparison of reflection coefficients by using third degree polynomial curve fit for all five beach positions. Only waves longer than the beach length are included and only the steepest waves with s = 1/60.

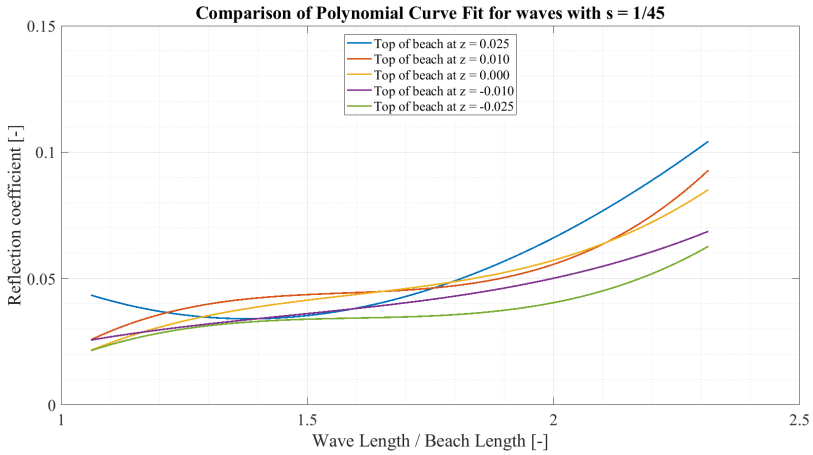

Figure A.22: Comparison of reflection coefficients by using third degree polynomial curve fit for all five beach positions. Only waves longer than the beach length are included and only the steepest waves with s = 1/45.

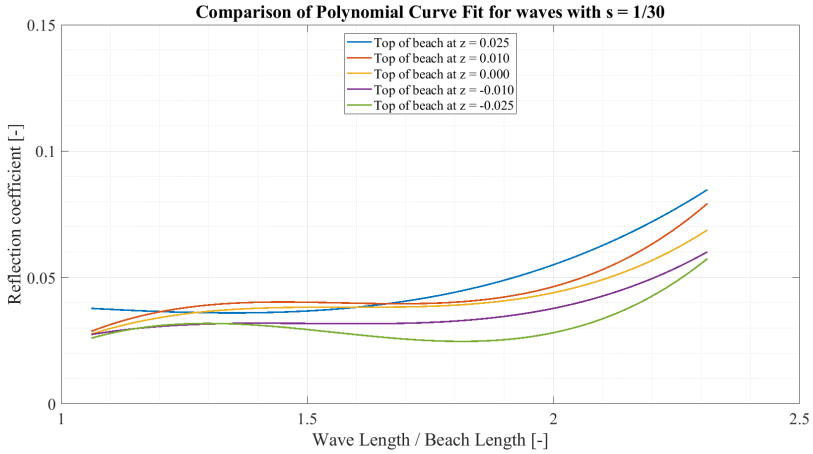

Figure A.23: Comparison of reflection coefficients by using third degree polynomial curve fit for all five beach positions. Only waves longer than the beach length are included and only the steepest waves with s = 1/30.

A.6 Polynomial curve fit for reflection coefficients for three wave steepnesses using Goda's method

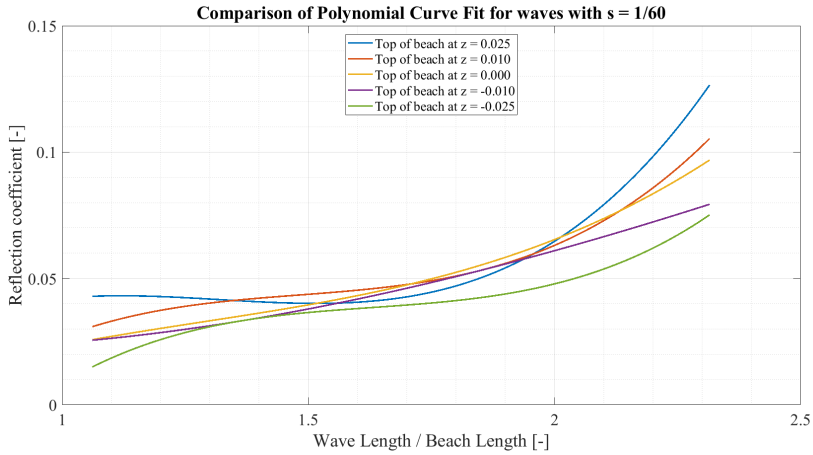

Figure A.24: Comparison of reflection coefficients by using third degree polynomial curve fit for all five beach positions. Only waves longer than the beach length are included and only the steepest waves with s = 1/60.

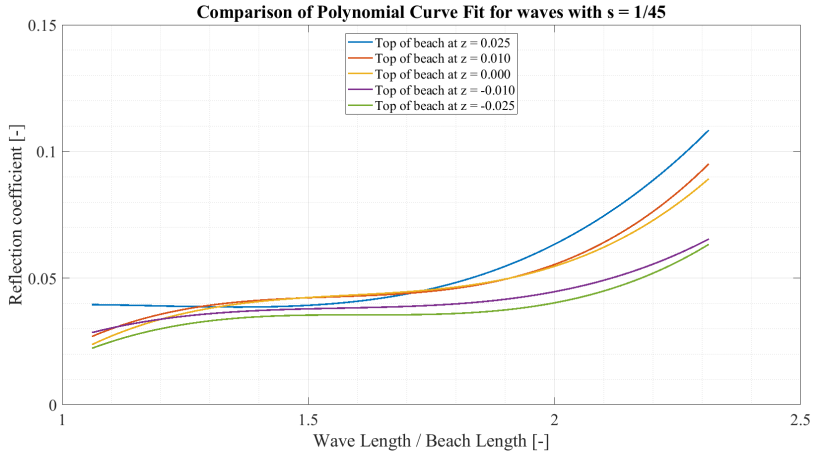

Figure A.25: Comparison of reflection coefficients by using third degree polynomial curve fit for all five beach positions. Only waves longer than the beach length are included and only the steepest waves with s = 1/45.

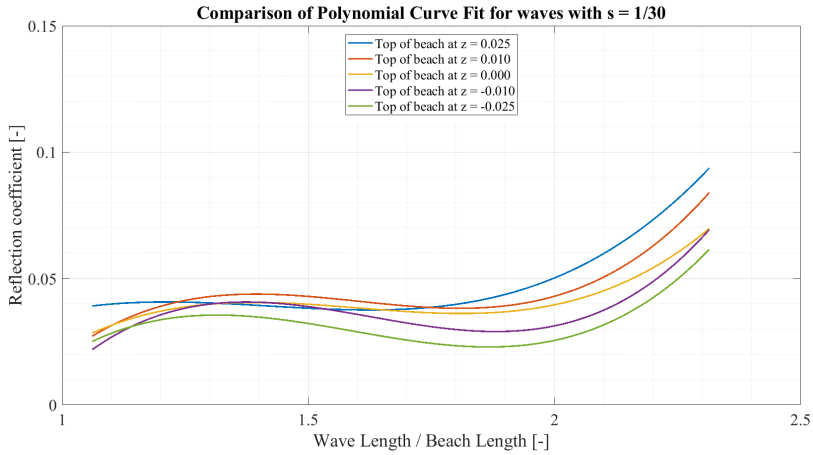

Figure A.26: Comparison of reflection coefficients by using third degree polynomial curve fit for all five beach positions. Only waves longer than the beach length are included and only the steepest waves with s = 1/30.

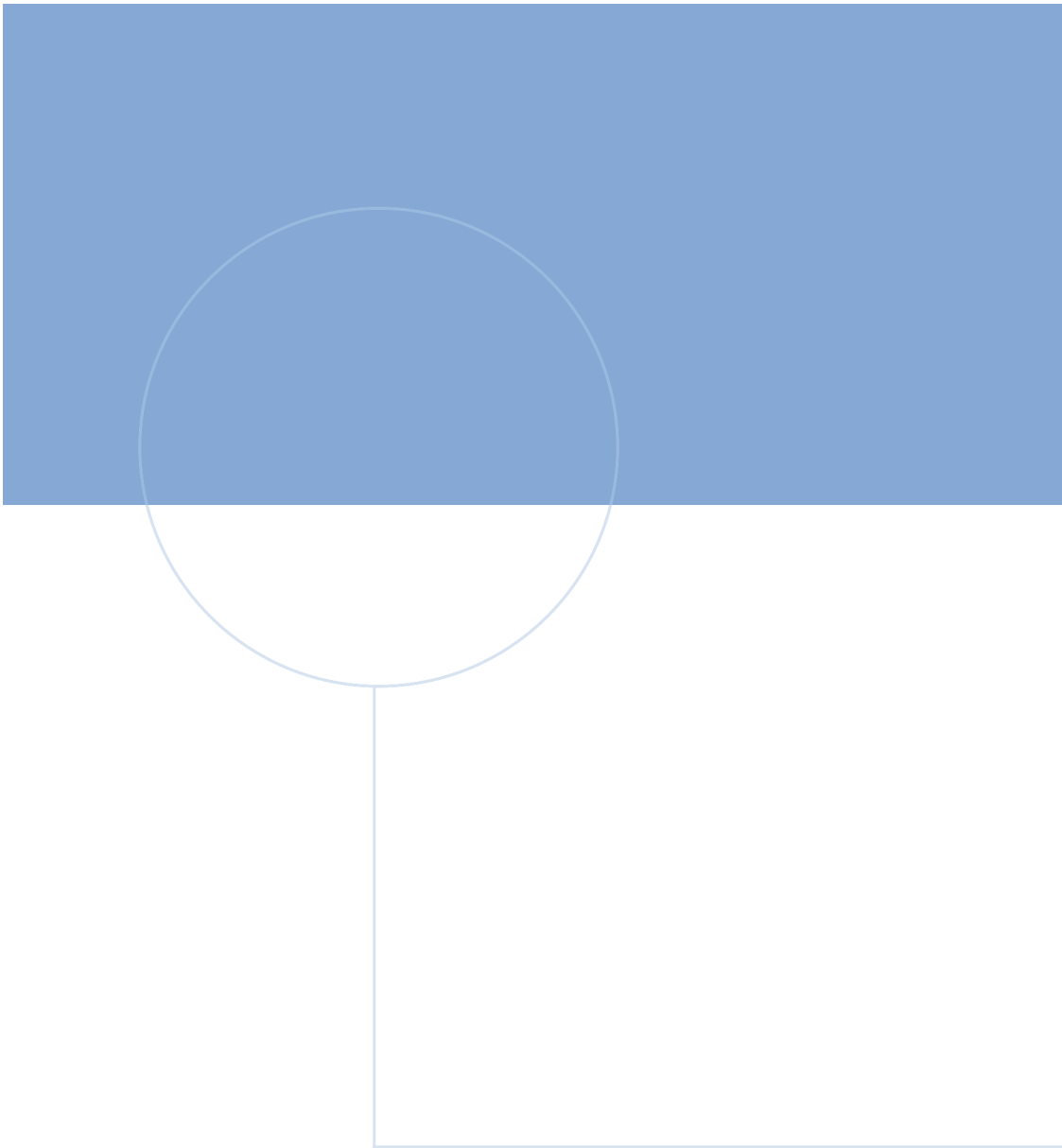

NTNU

Kunnskap for en bedre verden